

Radiative meson decay in the cloudy bag model

Paul Singer

Department of Physics, Technion-Israel Institute of Technology, Haifa, Israel

Gerald A. Miller

Institute for Nuclear Theory, Department of Physics, FM-15, University of Washington, Seattle, Washington 98195

(Received 14 May 1985)

We use the chiral $SU(2)_L \times SU(2)_R$ cloudy bag model to calculate magnetic dipole radiative transitions among pseudoscalar and vector mesons. A new picture for these decays emerges. Three different dynamical mechanisms, photon emission by quarks, photon emission from the pion cloud, and pion emission by mesonic bags accompanied by a transition from a vector bag to a photon, contribute singly or in combination to the 11 possible $M1$ transitions. The model accounts well for the observed rates. In particular, pion-cloud effects are necessary to explain the K^* decays.

I. INTRODUCTION

The radiative decays among vector (V) and pseudoscalar (P) mesons has continuously been a subject of considerable activity in particle physics. Following the pioneering theoretical work of Gell-Mann and others on $V \rightarrow P\gamma$ transitions^{1,2} and the early experiments of the 1960s which determined the $\omega \rightarrow \pi\gamma$ transition to have a partial decay width of the order of 1 MeV, a very large number of theoretical papers has been written on meson radiative decays. This theoretical proliferation has been matched by an extensive experimental effort. By now experimental results are available for practically all of the allowed transitions of the types $V \rightarrow P\gamma$ or $P' \rightarrow V'\gamma$ among the members of the lowest-lying multiplets. (These are the nonet of vector mesons and the octet and singlet of pseudoscalar mesons.) Although the experimental data for the various modes display a rather broad range of accuracies, it is possible to confront theory quantitatively with the fairly extensive experimental picture.³

In the present paper we limit our discussion to transitions of the type $V(J^P=1^-) \rightarrow P(J^P=0^-) + \gamma$ and $P'(J^P=0^-) \rightarrow V'(J^P=1^-) + \gamma$, which, according to multipole radiation rules, proceed via a magnetic dipole transition ($M1$). These transitions are, by far, the ones which have received most attention on both the experimental and theoretical sides. The continuing flow of theoretical papers on this subject is testimony to the fact that there is still no comprehensive theoretical picture, which explains satisfactorily the whole set of available data. A recent review⁴ of the field, although short of covering extensively the theoretical work in print, gives a good overview of the main lines of approach to this problem and we refer the interested reader to it. The conclusion evident from this review is that although some of the approaches which have been used are able to account for most transitions, there are always a few recalcitrant ones, usually the $K^* \rightarrow K\gamma$ decays, which do not integrate well into the overall picture.

In order to clarify the background, and set up the appropriate perspective for the rather different path we fol-

low in this paper to investigate the problem of radiative decays, we review succinctly the two principal lines of approach used in many different variants to deal with this problem. These are the constituent-quark-model approach and the phenomenological-Lagrangian approach within the $SU(3)$ -unitary-symmetry scheme.

In the constituent-quark model with pointlike u, d quarks of mass $\simeq 350$ MeV/ c^2 and strange quarks of mass $\simeq 500$ MeV/ c^2 , the matrix element of the $M1$ transition between the quark bound states V and P is expressed⁵ in terms of the magnetic moments μ_q of the quarks. Their magnitude is determined from the magnetic moments of the proton and neutron, which, in this picture,⁶ are also given in terms of quark magnetic moments. Using $SU(6)$ wave functions for the mesons involved, the partial decay widths of the various transitions are obtained. This original approach has been developed in numerous papers,⁴ for example, by improving⁷ on the quark wave functions or by using quark magnetic moments derived⁸ from fits to the measured magnetic moments of nucleons and hyperons or even by allowing the quarks to have arbitrary effective moments.⁹ In Table I we summarize the quark-model predictions in exact $SU(3)$ (column two), as well as in a broken- $SU(3)$ quark scheme which allows⁹ for *arbitrary* quark moments (column three), together with the experimental values (column six). The unbroken- $SU(3)$ -quark-model figures are calculated with equal u, d, s magnetic moments (as determined for u, d from the nucleonic moments) and with relativistic phase-space factors, as given in Ref. 4. The η, η' wave functions are taken to have equal amounts of strange quarks and ω (ϕ) to be composed purely of nonstrange (strange) quarks. It should be remarked that the quark magnetic moments used for deriving the $SU(3)$ -broken predictions, do not completely describe the observed hyperon moments.⁹

A second type of approach¹⁰⁻¹² uses effective Lagrangians,¹³ in which the basic VVP interaction is supplemented by vector-meson dominance of the hadronic electromagnetic current and symmetry relations. By allowing for $SU(3)$ breaking along the eighth component of the

TABLE I. The $M1$ radiative decay widths (in keV) calculated with the cloudy bag model are compared with previous calculations and with experiment.

Decay	Exact SU(3) ^a	Broken SU(3) ^b	MIT bag ^c	Present work (CBM)	Experiment ^d
$\omega \rightarrow \pi\gamma$	1200	861	310	1180	861 ± 76
$\rho \rightarrow \pi\gamma$	125	67	34	124	71 ± 10
$\phi \rightarrow \pi\gamma$	0	5.9	0	4.7	5.9 ± 2.2
$K^{*\pm} \rightarrow K^\pm \gamma$	71	96	8.7	47	51 ± 5
$K^{*0} \rightarrow K^0 \gamma$	275	139	94	98	75 ± 35^e
$\omega \rightarrow \eta\gamma$	8.6	4.4		2.3	3 ± 2
$\rho \rightarrow \eta\gamma$	78	57		23	55 ± 15
$\phi \rightarrow \eta\gamma$	226	57		43	51 ± 15
$\eta' \rightarrow \omega\gamma$	15	8.7		6.0	8.1 ± 2.8
$\eta' \rightarrow \rho\gamma$	142	108		53	87 ± 20^e
$\phi \rightarrow \eta'\gamma$	1.0	0.23		0.29	

^aIncluding ω_8 - ω_1 and η_8 - η_1 mixing, as explained in the text.

^bReference 9.

^cHackmann *et al.* (Ref. 19, Solution B)

^dReference 3.

^eSee also Ref. 61.

underlying strong interaction,¹⁴ the $M1$ electromagnetic transitions are expressed in terms of several parameters. Although a measured degree of success is achieved,¹⁰⁻¹² the additional freedom allowed by most general octet breaking is not sufficient to accommodate fully^{15,16} the observed pattern of decays and the fits achieved are usually comparable to those exemplified in Table I.

The present situation is thus unsatisfactory in two respects.

First, there is so far no theoretical description of one-photon radiative transitions of type $M1$ among pseudoscalar and vector mesons which succeeds in accounting for all the observed decay widths, even at the phenomenological level. Some of the many descriptions come quite close to this goal.^{4,17} These usually fail in some specific transitions, most often the K^* decays.

Second, and most important, the existing attempts have little or no motivation based on quantum chromodynamics. This is true both for the Lagrangian approach which deals directly with the hadronic states, as well as for the naive quark-model descriptions. Without belittling the wealth of physical understanding which these approaches have afforded over the years, it is certainly desirable to treat these electromagnetic transitions among hadrons from the perspective of an underlying theory of hadrons. Instead of searching for yet another improvement in the existing treatments, we attempt to investigate the problems by using a QCD approach to hadron physics. The $M1$ transitions are thus not divorced from other hadronic processes. One can use a single theoretical framework which accounts dynamically for the observed structure and spectroscopy of low-lying hadronic states as composites of quark and gluons, to describe the electromagnetic transitions among these same composite states. At the present stage of development, quantum chromodynamics does not provide yet a tool for quantitative exploration in the relatively low-energy region and one must resort to one of the models which have been developed to incorporate QCD basic features, the obvious candidate being the

bag model.¹⁸ However, when the MIT bag model¹⁸ was applied recently¹⁹ to the problems of mesonic $M1$ radiative transitions, in a first attempt to go beyond the "naive" quark model and its variations, it gave surprisingly poor results as can be seen from column four of Table I. For instance, the decays $\omega, \rho \rightarrow \pi\gamma$ came out as approximately one-third of the observed rate and the calculated $K^{*+} \rightarrow K^+\gamma$ mode is by an order of magnitude smaller than the experimental value.

In this paper we reconsider the problems of the mesonic $M1$ radiative transitions within the framework of the bag model;²⁰ however, we shall use a modern hybrid version which is endowed with chiral symmetry, the cloudy bag model²¹ (CBM). In this formulation, the pion is treated as a fundamental field interacting with pointlike quarks confined to a restricted volume of space. The coupling of the quantized pion field to quarks is introduced via a nonlinear realization of the chiral symmetry $SU(2)_L \times SU(2)_R$. The CBM has been used with remarkable success during the last few years to describe various strong and electromagnetic low-energy aspects of hadron physics. A very detailed and lucid account of these achievements, complemented by a comprehensive review of the basic MIT bag model and of various other hybrid bag models,²² is given in a recent review by Thomas.²³ Of particular relevance to our present work are the successful applications of CBM to the calculation of the magnetic moments of the baryon octet^{24,25} and to the calculation of three-meson strong vertices containing one or two pions.²⁶

The problem of obtaining a complete theoretical description of the observed magnetic moments of the baryon octet, bears in some ways close resemblance to the problems on hand of the $M1$ electromagnetic mesonic decays. Because of the common constituent quark description, the understanding of these two classes of physical quantities underwent a similar historical development. Moreover, as will be shown in this paper, the possible solution of the latter by a detailed analysis of quark dynamics and of the role of pion currents, uses the same

physical concepts that have been shown^{24,25} to overcome previous discrepancies in the analysis of baryon magnetic moments.

The early success of the constituent quark model in reproducing the magnetic moments of the proton, the neutron, and the Λ particle²⁷ has led to the premature belief that a simple SU(3) description of the moment of the baryon octet, including a heavier strange-quark mass, would be adequate. However, when accurate measurements of the Σ and Ξ moments became available, it became obvious that the simple approach is untenable. A recent analysis of the situation by Lipkin emphasizes²⁸ that "... present data indicate a serious disagreement with simple quark models for baryon magnetic moments which cannot be fixed up by symmetry breaking, relativistic corrections, configuration mixing, or quark-diquark models." By amending these words to appropriately describe the similar corrections to the symmetry results, used in the various analyses of the mesonic $M1$ transitions, Lipkin's statement is also quite suitable to characterize the present state of affairs concerning the radiative meson decays. It was only when the sizable effects of mesonic exchange currents²⁹ were included in the analysis, that a satisfactory description for the baryon magnetic moments emerged.^{24,25} The consideration of similar (and additional) effects, which arise when using the CBM as the basic tool for a description of $M1$ electromagnetic transitions among mesons, is the main objective of this paper.

Of more direct relevance to the present investigation is our recent calculation²⁶ of mesonic vertices involving one or two pions, i.e., $\omega\rho\pi$, $K^*K\pi$, $K^*K^*\pi$, $\rho\pi\pi$, in which we have shown that the CBM gives remarkably accurate values for these couplings. The successful calculation of these vertices allows an extension of our approach to electromagnetic transitions. Another essential ingredient, which plays an important role in the present approach, is the ability of the CBM to satisfactorily describe²⁶ the electromagnetic decays of the vector mesons.

When the CBM is applied to the $M1$ transitions a new picture for these decays emerges and the dynamics of the observed pattern of these decays is clarified. All previous descriptions used essentially a common mechanism for all of these transitions. (Examples are the defined interaction vertex of a phenomenological Lagrangian or a basic moment due to quark transitions, including, possibly, some symmetry breaking.) The use of SU(3) symmetry led to the well-known relations among the matrix elements of the various transitions. By explicitly treating the dynamics of quark and pions in the CBM, we find that the $M1$ transitions among pseudoscalar and vector mesons may be classified into three main groups. A separate physical mechanism dominates the transition matrix of each.

(1) The matrix elements for the decays of the type $V \rightarrow \eta\gamma$ or $\eta' \rightarrow V\gamma$, where V is any of the ω, ρ, ϕ mesons, are given by the contribution of the quark electromagnetic current inducing a radiative transition between $V \rightarrow \eta$ or $\eta' \rightarrow V$ bags. There are no contributions (to second order) from pion exchange to these transitions. [See Fig. 1(a).]

(2) The matrix elements for $K^* \rightarrow K\gamma$ charged and neutral decays are due to a combination of the quarks and

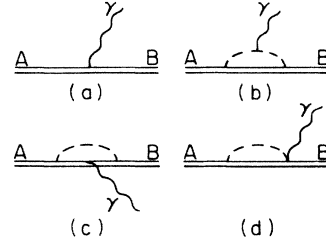


FIG. 1. In the cloudy bag model, a radiative transition from bag A to bag B contains several possible terms, (a), (b), (c), (d). The bags A, B are quark-antiquark states.

pion electromagnetic currents, inducing a radiative transition among K^* and K bags. The pion-exchange currents play a significant role in these transitions. [See Figs. 1(b)–1(d).]

(3) The decays with a pion in the final state, i.e., $\omega \rightarrow \pi\gamma$, $\rho \rightarrow \pi\gamma$, $\phi \rightarrow \pi\gamma$, are due to pion-induced transitions among ω and ρ bags with emission of an elementary pion, combined with the $\omega \rightarrow \gamma$ or $\rho \rightarrow \gamma$ transitions induced by the quark electromagnetic current. (See Fig. 2.)

This novel picture is related to the SU(2) \times SU(2) basic chiral symmetry of the CBM Lagrangian, emphasizing the singular role of the pion from among the pseudoscalar octet.^{30,31} Hence the matrix elements for various decays are not related by a straightforward application of the Wigner-Eckhart theorem utilizing the SU(3)-multiplet classification of mesons, as is usually done in treating these decays. Instead, specific dynamical mechanisms dictated by the CBM Lagrangian endowed with SU(2) \times SU(2) symmetry are needed to compute the transition rates. The calculation is performed to first order in electromagnetism and using an expansion in the pion field of the linearized σ model which provides the implementation of chiral symmetry in the Lagrangian. It is therefore not surprising that the picture emerging from our treatment differs significantly from the conventional one.

To better appreciate how our picture differs from previous ones it is worthwhile to consider the following question: Would the computations of the diagrams of Figs. 1 and 2 using relativistic Feynman diagrams and point particles give a good description of the decays? The answer is no, unless many more parameters are added. This can be seen from the decays of class 1, for which there are no pion contributions. For pointlike mesons, there would be no radiative decays unless one introduces a relativistic effective interaction, e.g., of the form

$$H_I = g_{VP} \epsilon_{\alpha\beta\gamma\delta} \partial_\alpha A_\beta \partial_\gamma V_\delta P,$$

where g_{VP} is the effective coupling constant for the radiative transition of a vector meson V to a pseudoscalar meson P . Without an underlying model to specify relationships between various decays there is, in principle, a different value of g_{VP} for every initial and final state.

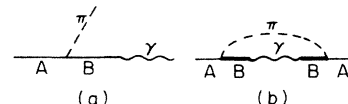


FIG. 2. The diagram contributing to pionic $M1$ radiative transitions in the cloudy bag model (a). In the actual calculation, (b) is used for reasons explained in the text.

The arbitrary nature of g_{VP} renders the “pointlike-particle model” essentially useless.

Only when one introduces an underlying (e.g., quark) model, do these ambiguities disappear. For example, Kokkedee’s book³² (Chap. 12) shows that the constants g_{VP} are known factors of the magnetic moment of a proton. Using those relationships, Table 8, evaluation of the Feynman graphs of Fig. 1(a), one gets a reasonable description of the class (1) decays. In the bag model, the magnetic moment is proportional to the bag size, so the composite nature of the hadron is essential.

There are several other possible procedures. One could use effective quark magnetic moment operators and very small bags, but one would have to account for the state dependence of such magnetic moments. Alternatively, one could use small bags, with small effective quark magnetic moments and rely solely on pionic effects. This could work for the decays of class (2), but would fail for class (1).

The utility of the cloudy bag model is that it combines the successful aspects of the quark model with necessary pion-cloud effects. The needed pion-hadron coupling constants are determined by the model. Using nucleon bag radii in the range 0.8–1 fm, and the mesonic radii related to those values by the bag model leads to good agreement with the radiative decays and other properties. This success is encouraging but, it is probably not unique to the cloudy bag model. For example, some form of a semirelativistic quark model, using reasonably large hadrons along with pionic effects appended in a manner consistent with PCAC (partial conservation of axial vector current), would probably be successful.

Needless to say, our picture is an approximate one, to the extent that the entire CBM formalism is only a model description of the QCD framework. The nature of the pion is a particularly intriguing one and there has been much interest lately in clarifying the connection between the possible $q\bar{q}$ structure and the Goldstone-boson facet of the pion as an agent of spontaneous breaking of the chiral symmetry.^{33–35} Hence, in a more complete formulation, one would have to include a detailed picture of the pion, beyond the elementary-field approximation of the cloudy bag model.

There is another possible problem associated with the cloudy bag model. The MIT Lagrangian does produce a $q\bar{q}$ state with the quantum numbers of the pion. If the quantized pion field were introduced in addition, the cloudy bag model would have two kinds of pions and difficulties with overcounting would arise. However, in the cloudy bag model there is only *one* pion: the quantized pion field. The bag pion state is projected out (removed) from the Hilbert space of states used for computations. The formal procedure to achieve this is discussed in detail in earlier papers,¹⁹ so only a brief discussion is presented here. One starts with the Lagrangian density, \mathcal{L}^{CBM} , and uses canonical techniques to obtain the corresponding Hamiltonian, H^{CBM} . Then, a truncated Hamiltonian is employed for practical calculations. That is, one makes the approximation

$$H^{\text{CBM}} \Rightarrow \sum_{\alpha\beta} |\alpha\rangle \langle \alpha| H^{\text{CBM}} |\beta\rangle \langle \beta| ,$$

where the prime indicates that only certain states of interest are kept in the sum over α and β . For example, for pion-nucleon scattering the states consisted of $|N\rangle, |\Delta\rangle$ and $a^\dagger(k)|N\rangle, a^\dagger(k)a^\dagger(k')|N\rangle$. The operator $a^\dagger(k)$ creates the quantized pion state. In the present work the states α, β consist of the bag states of the $\omega, \rho, \phi, K^{*\pm}, K^\pm, K^{*0}, K^0, \eta, \phi,$ and η' . In addition one uses the only quantized pion. The baglike pion never appears, so that, e.g., terms in which a ρ bag becomes a pion bag plus a photon do not enter. This is because neither α nor β is the bag pion. The judicious use of projection-operator techniques ensures that no overcounting arises. (To simplify the notation the truncation procedure is not mentioned below. Nonetheless it is employed in the calculations.) Of course, the ability to avoid a formal difficulty does not ensure success. Indeed, testing the assumption that the pion can be treated as a quantized field and not a bag is one of our main goals.

Another fundamental difficulty, associated with all bag models, is that Lorentz invariance is dropped in the process of evaluating matrix elements. There are many prescriptions available in the literature which seek to make the necessary “recoil” and “center-of-mass” corrections. None is truly satisfactory. As stated in Ref. 23, “to be honest, any of the four possible options is equally acceptable and one has to accept an uncertainty of at least $\pm 10\%$ on bag-model predictions of rms radii and magnetic moments . . . this is still considerably better than the uncertainties associated with relativistic corrections in the nonrelativistic quark models.”

This problem certainly occurs in our computations of the radiative decay widths, and one can ask if the problem is even more severe here. One may note that for $M1$ transitions the matrix elements for radiative decays are very similar to those of magnetic moments. Indeed, the quark contributions to radiative decays may be reduced to a magnetic moment computation in the limit $3j_1(qr) = qr$, where q is the photon momentum and r the quark position operator. Since the next-order term is $(q^2 r^2/10)$ and q is not very large, there is a close correspondence between these radiative-decay matrix elements and magnetic moments. Furthermore, nodeless $\kappa = -1$ quark wave functions are used for both mesons and baryons. Thus Thomas’s estimate of a 10% uncertainty applies at least approximately here. However, other matrix elements are more troublesome. For example, the matrix element for ω to $\pi\gamma$, Sec. IV D, does not look like a magnetic moment. The uncertainty in quantities like this is somewhat larger, since our treatment allows for the inclusion of transitions that do not actually occur.

The organization of this paper is as follows: Sec. II gives a concise formulation of the CBM. In Sec. III the electromagnetic field is introduced in the CBM Lagrangian and the expressions for the $M1$ transition moment between bags is given. Furthermore, the direct transitions between vector-meson bags and single photons are derived from the CBM formalism and their strength calculated. Expressions for the partial decay widths are also given here. In Sec. IV we present the detailed calculation of the various one-photon transitions among pseudoscalar and vector-meson states. Finally, Sec. V contains an analysis

of our results and a discussion of the approximations involved.

II. THE CLOUDY BAG MODEL

The success of the original MIT bag model¹⁸ was clouded by the lack of chiral symmetry in the MIT-bag Lagrangian. This is because the axial-vector current of the MIT Lagrangian is not conserved at the bag boundary. Since chiral symmetry plays an important role in low-energy hadron physics,^{30,31} it was obvious that the model should be amended so as to be endowed with this essential property. Chodos and Thorn²² and Inoue and Maskawa²² supplemented the MIT Lagrangian by a multiplet of (σ, π) fields,³⁶ coupled to the quarks at the bag surface, thus providing it with additional fields contributing to the axial-vector current. These fields have the role of restoring the chiral symmetry by allowing the axial-vector current at the bag surface to be continuous. This opened the era of the "hybrid bag models," with Lagrangians containing quarks, gluons, and "elementary" pions (and σ 's), which were proposed in a multitude of different formulations.^{22,23} In addition, by allowing for spontaneous symmetry breaking, the consequential massless Goldstone pseudoscalar boson is identified with the isotriplet pion field. The actual small mass of the pion brings about some breaking of the chiral symmetry, so that the axial current becomes partially conserved, its divergence fulfilling the famous PCAC relation.

In the cloudy bag model²¹ a nonlinear realization of the σ model is used, by employing the $SU(2) \times SU(2)$ invariant relation

$$\sigma^2 + \pi^2 = f^2 \quad (1)$$

to eliminate the σ field from the Lagrangian. The pion field, which is coupled to the quark fields at the bag surface, is allowed then to exist both inside and outside the bag. One may redefine³⁷ the Gell-Mann-Lévy fields with the aid of an isospin-triplet pseudoscalar field ϕ so that $(\hat{\phi} = \phi / f)$

$$\sigma = f \cos(\phi / f), \quad (2)$$

$$\pi = f \hat{\phi} \sin(\phi / f),$$

which fulfills (1). The CBM Lagrangian density, containing the MIT Lagrangian plus a nonlinear- σ -model part (from which the σ field is eliminated), reads²¹

$$\begin{aligned} \mathcal{L}_{\text{CBM}} = & \sum_q \left[\frac{i}{2} \bar{q}(x) \overleftrightarrow{D} q(x) - m_q \bar{q} q \right] \theta_v - B \theta_v \\ & - \frac{1}{4} F_{\mu\nu}^a F_a^{\mu\nu} \theta_v - \frac{1}{2} \sum_q \bar{q}(x) e^{i\tau \cdot \hat{\phi}(x) \gamma_5 / f} q(x) \Delta_s \\ & + \frac{1}{2} [\mathcal{D}_\mu \phi(x)]^2 + f^2 m_\pi^2 \{ \cos[\phi(x)/f] - 1 \}, \end{aligned} \quad (3)$$

where we have introduced possible quark masses and $\theta_v = 1$ (0) inside (outside) the bag volume. $q(x)$ is the quark field, B is the constant energy density term of the MIT bag, and Δ_s is a surface delta function. The gluon field tensor $F_{\mu\nu}^a$ is given by

$$F_{\mu\nu}^a = \partial_\mu G_\nu^a - \partial_\nu G_\mu^a + g f^{abc} G_\mu^b G_\nu^c, \quad (4)$$

where G_μ^a are the eight colored gluon fields, f_{abc} the $SU(3)$ structure constant, and g the strong coupling constant. The quark covariant derivative is defined

$$(D_\mu)_{\alpha\beta} = \partial_\mu \delta_{\alpha\beta} - ig \sum_a \frac{\lambda_{\alpha\beta}^a}{2} G_\mu^a, \quad (5)$$

where λ^a are the eight 3×3 matrices of $SU(3)$. We dropped indices whenever possible, for simplicity. Hence, $q(x)$ stands in fact for $q_m^a(x)$, where a and m are color and flavor indices, respectively. The covariant derivative \mathcal{D}_μ is given by

$$\mathcal{D}_\mu \phi = (\partial_\mu \phi) \hat{\phi} + f \sin(\phi/f) \partial_\mu \hat{\phi}. \quad (6)$$

It is evident that (3) reduces to the MIT Lagrangian for $\phi \rightarrow 0$.

The CBM is greatly simplified when the following assumptions are made:²¹ the $\phi(x)/f$ field is relatively small³⁷ and it can be used as an expansion quantity and furthermore, the quark wave function solution of the MIT bag is not sensibly distorted by the pion field. Then, to first order in an expansion in $\phi(x)/f$ one has (dropping, for simplicity, the gluon sector which we shall not use explicitly in this work)

$$\begin{aligned} \mathcal{L}_{\text{CBM}} = & \sum_q \left[\frac{i}{2} \bar{q}(x) \overleftrightarrow{D} q(x) - m_q \bar{q}(x) q(x) - B \right] \theta_v \\ & - \frac{1}{2} \sum_q \bar{q}(x) q(x) \Delta_s \\ & - \frac{i}{2f} \sum_q \bar{q}(x) \tau \cdot \hat{\phi}(x) \gamma_5 q(x) \Delta_s \\ & + \frac{1}{2} [\partial_\mu \phi(x)]^2 - \frac{1}{2} m_\pi^2 \phi(x)^2, \end{aligned} \quad (7)$$

and the equations of motion are

$$(i\partial - m)q(x) = 0, \quad x \in V, \quad (8a)$$

$$i\gamma \cdot n q(x) = q(x), \quad x \in S, \quad (8b)$$

$$B = -\frac{1}{2} n \cdot \partial \left[\sum_q \bar{q}(x) q(x) \right], \quad x \in S, \quad (9a)$$

$$(\partial^2 + m_\pi^2)\phi(x) = -\frac{i}{2f} \sum_q \bar{q}(x) \gamma_5 \tau q(x) \Delta_s. \quad (9b)$$

Most CBM calculations have employed this linearized form. The vector and axial-vector currents of this Lagrangian are

$$\mathbf{V}_\mu(x) = \frac{1}{2} \bar{q}(x) \gamma_\mu \tau q(x) \theta_v + \phi(x) \times \partial_\mu \phi(x), \quad (10)$$

$$\mathbf{A}_\mu(x) = \frac{1}{2} \bar{q}(x) \gamma_\mu \gamma_5 \tau q(x) \theta_v + f \partial_\mu \phi(x). \quad (11)$$

For $m_\pi \neq 0$ one obtains

$$\partial_\mu A^\mu(x) = -f m_\pi^2 \phi(x) \quad (12)$$

which enables one to identify f of Eq. (1), (3), (7), and (9b) with the pion decay constant

$$f \equiv f_\pi (=93 \text{ MeV}) . \quad (13)$$

We remark also that in the approximation leading to (7) and (9) the ϕ field is identical to the pion field of the σ model, Eq. (2).

The CBM Lagrangian is thus a sum of the MIT-bag Lagrangian, a free-pion term, and an interaction term. The effects of the pion field, which is quantized and used in an expansion in ϕ/f_π , are then treated as a perturbation on the MIT-model results. This is effected by working in a Hamiltonian formulation in the space of colorless bags to describe the known multiplets of hadrons. The CBM has been shown to account successfully for the coupling of pions to baryons^{21,38,39} and mesons²⁶ as well as for a variety of low-energy hadron-physics processes and properties, as summarized in Refs. 23 and 38.

Although many of the CBM results were obtained using the formulation presented above, an alternative formulation of the CBM exists which exhibits a pseudovector coupling of quarks to pions throughout the volume of the bag, as opposed to the pseudoscalar couplings of Eq. (7) which is limited to the bag surface.

The alternative formulation^{39,40} is obtainable from (3) by a unitary transformation on the quark field

$$Sq(x) = q_N(x) = \exp(i\tau \cdot \phi \gamma_5 / 2f_\pi) q(x) . \quad (14)$$

The Lagrangian expressed in terms of the "new" quark

field $q_N(x)$ is then (in the quark and pion sector)

$$\begin{aligned} {}^N\mathcal{L}_{\text{CBM}}(x) = & \sum_{q_N} \left[\frac{i}{2} \bar{q}_N \not{D} q_N - m_q \bar{q}_N q_N - B \right] \theta_v \\ & - \frac{1}{2} \bar{q}_N q_N \Delta_s + \frac{1}{2} (\mathcal{D}_\mu \phi)^2 \\ & + f_\pi^2 m_\pi^2 [\cos(\phi/f_\pi) - 1] \\ & + \frac{1}{2f_\pi} \bar{q}_N \gamma^\mu \gamma_5 \tau q_N \cdot (\mathcal{D}_\mu \phi) \theta_v , \end{aligned} \quad (15)$$

where $\mathcal{D}_\mu \phi$ is defined in Eq. (6) and the covariant derivative acting on the quark field is now

$$\not{D} q_N(x) = \not{\partial} q_N(x) - \frac{i}{2} [\cos(\phi/f_\pi) - 1] \tau \cdot (\hat{\phi} \times \hat{\partial} \phi) q_N(x) . \quad (16)$$

The volume pseudovector coupling is explicit in (15). One should note that in this pseudovector formulation, the linear boundary condition for quarks is the same as in the MIT bag model. It does not depend on the meson field.

If we expand (15) in ϕ/f_π , keeping also the second-order term which arises from the covariant derivative (16) on the quark fields, one obtains

$$\begin{aligned} {}^N\mathcal{L}_{\text{CBM}} = & \sum_{q_N} \left[\left[\frac{i}{2} q_N \overleftrightarrow{\not{\partial}} q_N - m_q \bar{q}_N q_N - B \right] \theta_v - \frac{1}{2} \bar{q}_N q_N \Delta_s \right. \\ & \left. + \left[-\frac{1}{4f_\pi^2} \bar{q}_N \gamma^\mu \tau q_N \cdot (\phi \times \partial_\mu \phi) + \frac{1}{2f_\pi} \bar{q}_N \gamma^\mu \gamma_5 \tau q_N \cdot \partial_\mu \phi \right] \theta_v \right] + \frac{1}{2} (\partial_\mu \phi)^2 - \frac{1}{2} m_\pi^2 \phi^2 . \end{aligned} \quad (17)$$

In this form, the results of current algebra for pion scattering on hadrons are immediately derivable.³⁹⁻⁴¹ It is also the appropriate form to be used in the derivation²⁶ of mesonic strong vertices containing two pions, while for processes involving one pion the formulations (7) and (17) are equivalent.

In order to calculate various hadronic processes, it is useful to reexpress the CBM equation in terms of a Hamiltonian. First, one uses (17) to derive the quark Hamiltonian

$$\begin{aligned} H &= \int d^3x T^{00}(x) , \\ T^{\mu\nu}(x) &= \sum \frac{\partial \mathcal{L}}{\partial (\partial_\mu \psi)} \partial^\nu \psi - g^{\mu\nu} \mathcal{L}(x) . \end{aligned}$$

The quark interaction Hamiltonian has two terms, expressing the basic coupling to one and two pions,

$$\begin{aligned} H_{\text{int}} = & \int d^3x \frac{1}{2f_\pi} \sum_q \left[\bar{q}_N \gamma^\mu \gamma_5 \tau \cdot q_N \partial_\mu \phi \right. \\ & \left. - \frac{1}{2f_\pi} \bar{q}_N \gamma^\mu \tau \cdot q_N (\phi \times \partial_\mu \phi) \right] . \end{aligned} \quad (18)$$

The isotopic spin invariance obviously requires that only the u and d quarks contribute to the interaction terms of (17) and (18). In the following we drop the subscript N . The direct coupling to two pions is essential in getting^{26,40} the correct current-algebra results from the CBM Lagrangian.

It is useful to present a few expressions needed to evaluate the influence of H_{int} . The pion-field expansion is

$$\phi_j(\mathbf{r}, t=0) = \int \frac{d^3k}{[2\omega_k(2\pi)^3]^{1/2}} \times [a_j(\mathbf{k})e^{i\mathbf{k}\cdot\mathbf{r}} + a_j^\dagger(\mathbf{k})e^{-i\mathbf{k}\cdot\mathbf{r}}], \quad (19)$$

with

$$\begin{aligned} [a_j(\mathbf{k}), a_{j'}(\mathbf{k}')] &= [a_j^\dagger(\mathbf{k}), a_{j'}^\dagger(\mathbf{k}')] = 0, \\ [a_j(\mathbf{k}), a_{j'}^\dagger(\mathbf{k}')] &= \delta_{jj'} \delta^{(3)}(\mathbf{k} - \mathbf{k}'). \end{aligned} \quad (20)$$

$$N_i^2 = \frac{1}{4\pi R^3 j_0^2(\Omega_i)} \frac{(\alpha_i^-)^2 (\Omega_i^2 + m_i^2 R^2)}{2(\Omega_i^2 + m_i^2 R^2)^{1/2} [(\Omega_i^2 + m_i^2 R^2)^{1/2} - 1] + m_i R}. \quad (21c)$$

The quark frequency is determined by the linear boundary condition at the bag radius $r = R$

$$\alpha_i^- j_1(\Omega_i) = \alpha_i^+ j_0(\Omega_i). \quad (22)$$

The first term of (18) can then be rewritten making use of Eqs. (19)–(22) as

$$H_I^{(q)} = \sum_j \int d^3k [V_j^q(\mathbf{k}) a_j(\mathbf{k}) + V_j^{q\dagger}(\mathbf{k}) a_j^\dagger(\mathbf{k})] \quad (23)$$

with

$$V_j^q(\mathbf{k}) = \sum_{i=1}^3 i f_{Q_i} \frac{u(kR)}{[2\omega_k(2\pi)^3]^{1/2}} b_i^+ \boldsymbol{\sigma} \cdot \mathbf{k} \tau_j b_i, \quad (24)$$

where b_i are the spin-isospin wave functions of the quarks and

$$f_{Q_i} = \frac{\Omega_i^2}{3f_\pi [2\alpha_i(\alpha_i - 1) + m_i R]}, \quad (25a)$$

$$\alpha_i = (\Omega_i^2 + m_i^2 R^2)^{1/2}, \quad (25b)$$

$$u(kR) = j_0(kR) + j_2(kR). \quad (25c)$$

We have added the superscript (q) to the H_I of Eq. (23) to underline that this term is written in the space of quarks, which are of three flavor varieties u , d , and s in our treatment.

Most applications of the CBM have been carried out by evaluating H_{int} in the space of colorless hadrons. This is done by sandwiching H_{int} between the hadronic states. Note that the bag-model pion state never appears in our formulation. For the present application, it is simpler to work with Eq. (23) directly.

III. ELECTROMAGNETIC INTERACTIONS IN THE CLOUDY BAG MODEL

In this section we describe the electromagnetic interactions in the cloudy bag model. Then we present the various expressions needed for the calculations of radiative transitions between vector and pseudoscalar bags, and the electromagnetic transitions of vector bags to pions. Whenever possible, we follow the notation of Ref. 24, in which the CBM is used to discuss the static electromagnetic properties of baryons.

The MIT bag solution²¹ for the quarks is

$$q_i(\mathbf{r}, t=0) = N_i \begin{bmatrix} \alpha_i^+ j_0(\Omega_i r/R) \\ i\alpha_i^- j_1(\Omega_i r/R) \boldsymbol{\sigma} \cdot \hat{\mathbf{r}} \end{bmatrix} b_i \theta(R-r) \quad (21a)$$

with

$$\alpha_i^\pm = \left[\frac{(\Omega_i^2 + m_i^2 R^2)^{1/2} \pm m_i R}{(\Omega_i^2 + m_i^2 R^2)^{1/2}} \right]^{1/2} \quad (21b)$$

and N_i the normalization constant given by

A. The electromagnetic current

The electromagnetic interaction is added to the CBM Lagrangian (17) via the minimal coupling substitution $\partial_\mu \rightarrow \partial_\mu - ie_a A_\mu$ with A_μ representing the photon field, whenever ∂_μ is acting on a charged field with electric charge e_a . Disregarding the pionic contact term $e^2 A_\mu A^\mu \phi^* \phi$ which is of second order in electromagnetism, the interaction term of the Lagrangian has the form

$$\mathcal{L}_{\text{int}}^{(\text{em})}(x) = j_\mu(x) A^\mu(x) \quad (26)$$

with the electromagnetic hadronic current $j_\mu(x)$ given by

$$j_\mu(x) = j_\mu^Q(x) + j_\mu^\pi(x) + j_\mu^{\pi\pi Q}(x) + j_\mu^{\pi Q}(x). \quad (27)$$

There is thus a quark contribution to the current denoted by $j_\mu^Q(x)$, a pionic contribution $j_\mu^\pi(x)$, and two contact terms $j_\mu^{\pi\pi Q}(x)$ and $j_\mu^{\pi Q}(x)$, representing $qq\pi\pi\gamma$ and $qq\pi\gamma$ vertices, respectively. The latter terms arise from the second line of (17), when introducing minimally the electromagnetic field. The explicit expressions for the four parts of $j_\mu(x)$ are

$$j_\mu^Q(x) = \sum_i e_i \bar{q}_i(x) \gamma_\mu q_i(x) \theta_v, \quad (28)$$

$$j_\mu^\pi(x) = ie [\phi^*(x) \partial_\mu \phi(x) - \phi(x) \partial_\mu \phi^*(x)], \quad (29)$$

$$j_\mu^{\pi\pi Q}(x) = -\frac{ie}{2f_\pi} \sum_i \bar{q}_i \gamma_\mu \gamma_5 (\tau^+ \phi^* - \tau^- \phi) q_i \theta_v, \quad (30)$$

$$j_\mu^{\pi Q}(x) = \frac{e}{4f_\pi^2} \sum_i \bar{q}_i \gamma_\mu (\tau^+ \phi^* \phi_3 + \tau^- \phi \phi_3 - 2\tau_3 \phi \phi^*) \times q_i \theta_v, \quad (31)$$

where i stands for the quark degrees of freedom and $\phi = (\phi_1 + i\phi_2)/\sqrt{2}$ is the operator which creates positive pions and annihilates negative pions [Eq. (19)]. Since our Lagrangian (17) arises from an expansion in ϕ/f_π and we do not study here phenomena intrinsically connected to two pions (like²⁶ $\rho \rightarrow 2\pi$, $\rho \rightarrow 2\pi\gamma$), the contribution of (31), which is of order f_π^{-2} , is neglected.

The explicit expressions for (28)–(30) are then obtained by using (19) for the pion field and Eq. (21), the static MIT bag solutions, for the quarks. The Coulomb gauge, $\nabla \cdot \mathbf{A} = 0$, is employed so we need only the spatial parts of the hadronic currents. These are

$$\mathbf{j}^Q(\mathbf{r}) = \sum_i e_i N_i^2 \frac{2\Omega_i}{\alpha_i} j_0 \left[\frac{\Omega_i \mathbf{r}}{R} \right] j_1 \left[\frac{\Omega_i \mathbf{r}}{R} \right] b_i^\dagger \boldsymbol{\sigma} \times \mathbf{r} b_i \cdot \boldsymbol{\theta}(R-r), \quad (32)$$

$$\mathbf{j}^\pi(\mathbf{r}) = \frac{ie}{2} \sum_{j,j'} \epsilon_{jj'3} \int \frac{d^3k d^3k'}{(2\pi)^3(\omega\omega')^{1/2}} [a_{j'}(-\mathbf{k}') + a_{j'}^\dagger(\mathbf{k}')] [a_j(\mathbf{k}) + a_j^\dagger(-\mathbf{k})] e^{i(\mathbf{k}-\mathbf{k}')\mathbf{r}}, \quad (33)$$

$$\begin{aligned} \mathbf{j}^\pi Q(\mathbf{r}) = & -\frac{ie}{2f_\pi} \sum_i N_i^2 \left[j_0^2 \left[\frac{\Omega_i \mathbf{r}}{R} \right] - j_1^2 \left[\frac{\Omega_i \mathbf{r}}{R} \right] \right] \\ & \times \int \frac{d^3k b_i^\dagger}{(2\pi)^{3/2}\omega^{1/2}} \{ \tau^+ [a_+(\mathbf{k})e^{i\mathbf{k}\cdot\mathbf{r}} + a_-^\dagger(\mathbf{k})e^{-i\mathbf{k}\cdot\mathbf{r}}] \\ & - \tau^- [a_-(\mathbf{k})e^{i\mathbf{k}\cdot\mathbf{r}} + a_+^\dagger(\mathbf{k})e^{-i\mathbf{k}\cdot\mathbf{r}}] \} \boldsymbol{\sigma} b_i \boldsymbol{\theta}(R-r). \end{aligned} \quad (34)$$

The creation and annihilation operators for charged pions, used in (34), are

$$\begin{aligned} a_\pm(\mathbf{k}) &= \frac{a_1(\mathbf{k}) \mp ia_2(\mathbf{k})}{\sqrt{2}}, \\ a_\pm^\dagger(\mathbf{k}) &= \frac{a_1^\dagger(\mathbf{k}) \pm ia_2^\dagger(\mathbf{k})}{\sqrt{2}}. \end{aligned} \quad (35)$$

B. The matrix elements of $V \rightarrow P\gamma$ transitions

The matrix element for a radiative transition from a vector to a pseudoscalar meson state, as obtained from (26) is

$$M_{PV} \equiv \left\langle P \left| \int d^3r \mathbf{j} \cdot \hat{\boldsymbol{\epsilon}} e^{-i\mathbf{q}\cdot\mathbf{r}} \right| V \right\rangle, \quad (36)$$

where \mathbf{j} is the electromagnetic current given in the CBM by (27) and $\hat{\boldsymbol{\epsilon}}$ is the polarization vector of the emitted photon, having three-momentum q in the rest frame of V . For the decays of a heavy pseudoscalar (η') to $V + \gamma$, the roles of P and V are interchanged. For P and V we take static bags, except when P is a pion, which is an elementary quantum field in our approach.

The physical decays occur between momentum eigenstates, so that in an exact calculation one should express these eigenstates in terms of the static bag states.^{26,42} For the decays between bags discussed here, of moderate momentum transfer, it is a reasonable approximation to perform a "static" calculation. Any momentum dependence arising from the construction of bags from momentum wave packets is therefore neglected. The reliability of this static approximation, and the particular case of $V \rightarrow \pi + \gamma$ decays, is the object of further discussion in Sec. V.

The most general matrix element describing an $M1$ transition $V \rightarrow P + \gamma$, obeying the requirements of parity and time-reversal invariance, is required to have in the rest system of the V the form

$$M_{PV} \sim F(q^2) \mathbf{S}_V \cdot (\hat{\boldsymbol{\epsilon}} \times \mathbf{q}), \quad (37)$$

where \mathbf{S}_V is proportional to the spin of the vector meson and $F(q^2)$ is a function of the momentum transfer q^2 . A similar form results for the decays $P' \rightarrow V + \gamma$ in the rest

frame of P' . Such expressions will eventually obtain from (36), after using explicit representations for the operators and wave functions involved. Denoting

$$\mathbf{K} = \hat{\boldsymbol{\epsilon}} \times \mathbf{q} \quad (38)$$

we also define for future use an effective matrix element μ_{PV} between P and V states for the magnetic dipole radiative transition. Using spherical vector components one has

$$\begin{aligned} M_{PV} &= \sum_n \langle 1m_V 1n | 00 \rangle iK_n^* \mu_{PV} \\ &= \frac{(-1)^{1-m_V}}{\sqrt{3}} iK_{-m_V}^* \mu_{PV} = -\frac{i}{\sqrt{3}} K_{m_V} \mu_{PV}, \end{aligned} \quad (39)$$

where

$$\mu_{PV} = \langle P | \boldsymbol{\Sigma} | V \rangle \quad (40)$$

with $\boldsymbol{\Sigma}$ being a pseudovector of spin properties and we have used

$$\langle 1m_V 1n | 00 \rangle = [(-1)^{1-m_V} / \sqrt{3}] \delta_{n, -m_V}.$$

The decay widths are to be calculated with the relativistic phase-space factor. Using the matrix element defined in (39) and (40), one finds that the decay widths $\Gamma_{V \rightarrow P\gamma}$, $\Gamma_{P \rightarrow V\gamma}$ are given by

$$\Gamma_{V \rightarrow P\gamma} = \frac{e^2 \mu_{PV}^2 q^3}{9\pi}, \quad (41)$$

$$\Gamma_{P \rightarrow V\gamma} = \frac{e^2 \mu_{PV}^2 q^3}{3\pi}, \quad (42)$$

where the relative momentum q is $q = (m_V^2 - m_P^2)/2m_V$ in $V \rightarrow P\gamma$ and $q = (m_P^2 - m_V^2)/2m_P$ in $P \rightarrow V\gamma$ decays.

Turn now to the explicit expressions of M_{PV} . The various contributing terms of $j_\mu(x)$ of Eq. (27), are denoted as M_{PV}^Q (the quark contribution), M_{PV}^π (the pionic contribution), $M_{PV}^{\pi Q}$ (the pion-quark contact-term contribution). We shall use the formalism of the cloudy bag model within the same framework as pioneered in Refs. 21 and 24, namely, we consider only terms having no more than

“one pion in the air” when the photon is emitted by the bag. Hence, in general, an electromagnetic transition between bags A and B will involve the several possible terms of Fig. 1.

$$\begin{aligned} M_{PV}^0 &= \left\langle P \left| \int_0^R d^3r j^Q \cdot \hat{\mathbf{e}} e^{-iq\cdot r} \right| V \right\rangle \\ &= \left\langle P \left| \sum_i e_i N_i^2 \frac{2\Omega_i}{\alpha_i} \int_0^R r^2 dr j_0 \left[\frac{\Omega_i r}{R} \right] j_1 \left[\frac{\Omega_i r}{R} \right] \int d\hat{\mathbf{r}} \hat{\mathbf{e}} \cdot (\boldsymbol{\sigma}_i \times \hat{\mathbf{r}}) e^{-iq\cdot r} \right| V \right\rangle. \end{aligned} \quad (43)$$

The angular integration gives

$$\int d\hat{\mathbf{r}} \hat{\mathbf{e}} \cdot (\boldsymbol{\sigma} \times \hat{\mathbf{r}}) e^{-iq\cdot r} = 4\pi i j_1(qr) \hat{\mathbf{q}} \cdot (\boldsymbol{\sigma} \times \hat{\mathbf{e}}).$$

If we define

$$\begin{aligned} \mu_i(q) &= \int_0^R dr \frac{4\pi r^3}{3} \frac{3j_1(qr)}{qr} N_i^2 \frac{2\Omega_i}{\alpha_i} j_0 \left[\frac{\Omega_i r}{R} \right] \\ &\quad \times j_1 \left[\frac{\Omega_i r}{R} \right] \end{aligned} \quad (44)$$

the final expression for M_{PV}^0 becomes

$$M_{PV}^0 = i \left\langle P \left| \sum_i \frac{e_i}{e} \mu_i(q) \boldsymbol{\sigma}_i \cdot \mathbf{K} \right| V \right\rangle, \quad (45)$$

where the quark component of the V - P magnetic transition μ_{PV} of Eq. (40) is

$$\mu_{PV}^0 = \left\langle P \left| \sum_i \frac{e_i}{e} \mu_i(q) \boldsymbol{\sigma}_i \right| V \right\rangle \quad (46)$$

with $\mu_i(q)$ given in (44). We see that M_{PV}^0 and μ_{PV}^0 conform to the general forms anticipated in (37) and (40). Note that Eq. (44) is exact and no “long-wavelength approximation” is made.

D. The pion contribution to M_{PV}

In this section we consider the “proper” pion term M_{PV}^π as well as the pion-quark contact term $M_{PV}^{\pi Q}$. From the explicit expression (34) for j^π one can see that this contribution is proportional to the integral of

$$r \left[j_0^2 \left[\frac{\Omega_i r}{R} \right] - j_1^2 \left[\frac{\Omega_i r}{R} \right] \right]$$

over the bag’s volume. As the eigenvalue equation for s -

$$\left[\frac{1}{2f_\pi R} \frac{\Omega}{\Omega-1} \right]^2 \frac{j_1(kR)j_1(k'R)}{(2\pi)^3 \sqrt{4\omega_k \omega_{k'}}} \left[\boldsymbol{\sigma} \cdot \hat{\mathbf{k}} \boldsymbol{\sigma} \cdot \hat{\mathbf{k}}' \tau_j \tau_{j'} \frac{1}{(\omega_k + \omega_{k'})\omega_{k'}} + \boldsymbol{\sigma} \cdot \hat{\mathbf{k}}' \boldsymbol{\sigma} \cdot \hat{\mathbf{k}} \tau_{j'} \tau_j \frac{1}{(\omega_k + \omega_{k'})\omega_k} \right].$$

The full expression for the pion contribution is found after some algebra to be

$$M_{PV}^\pi = \left\langle P \left| \sum_{i=1,2} \frac{-ie}{16\pi^3} \left[\frac{\Omega}{\Omega-1} \frac{1}{2f_\pi R} \right]^2 \int d^3k \frac{j_1(kR)j_1(k'R) \mathbf{k} \cdot \hat{\mathbf{e}} \boldsymbol{\sigma}_i \cdot (\hat{\mathbf{k}} \times \hat{\mathbf{k}}') \tau_3^i}{(\omega_k \omega_{k'})^2} \right| V \right\rangle. \quad (49)$$

We define now, remembering that $\mathbf{q} = \mathbf{k} - \mathbf{k}'$,

C. The quark contribution to M_{PV}

The quark contribution to the $V \rightarrow P\gamma$ transition is given by (32) and (36) as

wave massless quarks is $j_0 = j_1$ at the bag surface, and the integrand for the dipole matrix element is weighted by $j_1(qr)$, one may reasonably expect the contribution of this term to be generally quite small.⁴³ We therefore disregard it in the following. We are then left for the pionic contribution with

$$M_{PV}^\pi = \left\langle P \left| \int d^3r j^\pi \cdot \hat{\mathbf{e}} e^{-iq\cdot r} \right| V \right\rangle, \quad (47)$$

where $j^\pi(x)$ is given in (33), this contribution being represented diagrammatically in Fig. 1(b). The explicit evaluation of (47) involves the use of Eqs. (18)–(25).

In previous work we computed²⁶ meson-pion (e.g., $K^*K\pi$) coupling constants. The hadronic representation was employed to facilitate comparisons with experiment. The constants so obtained did agree with experimental values. Here we use Eq. (23) which uses a quark basis. This simplifies the present computations. The various π -coupling constants are not used explicitly in the present calculation. However the theory is the same as in Ref. 26. Thus the (more or less) correct coupling constants are used.

The basic quark-pion interaction is given in Eq. (18). For the first term of (18) which is of interest here, and to the order in ϕ/f_π at which we work, the pseudovector and pseudoscalar formulations are essentially equivalent.⁴⁴ Taking zero-mass u and d quarks and using $\rho[j_0(\rho) + j_2(\rho)] = 3j_1(\rho)$, we rewrite the quark-pion interaction term (24) as

$$V_j^q(\mathbf{k}) = \frac{i}{2f_\pi} \frac{\Omega}{\Omega-1} \frac{1}{kR} \frac{j_1(kR)}{[2\omega_k(2\pi)^3]^{1/2}} \boldsymbol{\sigma} \cdot \mathbf{k} \tau_j. \quad (48)$$

There are four terms in M_{PV}^π , involving bilinear products of pion creation and annihilation operators [see Eq. (33)], of which the general form is [we write here the term multiplying $a_j(-\mathbf{k}')a_j(\mathbf{k})\epsilon_{jj'3}$]:

$$\mathbf{P} = \mathbf{k} - \frac{\mathbf{q}}{2} = \mathbf{k}' + \frac{\mathbf{q}}{2} \quad (50)$$

and we rearrange the vectors in (49) to conform with (37). The pionic current contribution is then given by

$$M_{PV}^\pi = \frac{-i}{\sqrt{3}} (\hat{\mathbf{e}} \times \mathbf{q})_{m_V} \left\langle P \left| \sum_{i=1,2} (\sigma_3 \tau_3)_i \right| V \right\rangle W, \quad (51)$$

where

$$W = \frac{e}{27\pi^2} \left[\frac{\Omega}{2f_\pi(\Omega-1)} \right]^2 e^{-q^2 R^2/20} \int_0^\infty \frac{P^4 e^{-P^2 R^2/5} dP}{\left[\left(P^2 - \frac{q^2}{4} \right)^2 + m_\pi^2 \left(2P^2 + \frac{q^2}{2} \right) + m_\pi^4 \right]}. \quad (52)$$

In deriving (52) we have used an approximation

$$3j_1(kR) \simeq kRe^{-k^2 R^2/10} \quad (53)$$

known to be very accurate.²¹ Again, the expression obtained now for M_{PV}^π has the general required form of (37). Within the order of our approximation, we have also the term corresponding to Fig. 1(c) where the j^Q operates between states with "one pion in the air." It will be shown that this term is much less relevant than the term corresponding to Figs. 1(a) and 1(b).

E. Transitions involving pions in the final state

The treatment presented so far is suitable for discussing $M1$ electromagnetic transitions between vector and pseudoscalar bags, to which the decay modes $V \rightarrow \pi\gamma$ do not belong. So far, the elementary pions have entered the formalism via their contribution as virtual quanta (or "exchange currents"), as in Figs. 1(b), 1(c), and 1(d). The magnetic dipole transitions $V \rightarrow P\gamma$, listed in Table I, include, however, the channels $\omega \rightarrow \pi\gamma$, $\rho \rightarrow \pi\gamma$, and $\phi \rightarrow \pi\gamma$ which cannot be treated by the general formalism of transitions between bags. Most interestingly, these transitions are also induced by the CBM Lagrangian (17) with electromagnetic interactions (26) and (27), and occur as transitions among $\omega(\phi)$ and ρ bags with the emission of a real ("fundamental") pion, followed by a transition $\omega \rightarrow \gamma$ or $\rho \rightarrow \gamma$. The transitions $\omega, \rho, \phi \rightarrow \pi\gamma$ are depicted in Fig. 2.

The electromagnetic transitions of vector-meson bags to photon are the same ones which are responsible for the leptonic decays of vector mesons ($V \rightarrow l^+ l^-$) and have been formulated in the bag model by Duck⁴⁵ and treated recently by ourselves.²⁶ The relevant matrix elements between the vector meson and the vacuum are defined

$$\begin{aligned} \langle \rho(\mathbf{p}, m) | \bar{q}(x) \frac{1}{2} \tau \gamma^\mu q(x) | 0 \rangle \\ = \frac{m_\rho^2}{f_\rho} \epsilon_{(\rho)}^\mu(\mathbf{p}, m) \exp(-i\mathbf{p} \cdot \mathbf{x}), \end{aligned} \quad (54a)$$

$$\begin{aligned} \langle \omega(\mathbf{p}, m) | \frac{1}{\sqrt{3}} \bar{q}(x) \gamma^\mu q(x) | 0 \rangle \\ = \frac{m_\omega^2}{f_\omega} \epsilon_{(\omega)}^\mu(\mathbf{p}, m) \exp(-i\mathbf{p} \cdot \mathbf{x}), \end{aligned} \quad (54b)$$

for vector mesons ρ, ω of momentum \mathbf{p} and spin m .

The definitions (54) require that Lorentz-invariant state vectors be used, and this presents difficulties in using bag models to evaluate f_ρ and f_ω . Bag-model eigenstates violate Lorentz invariance, so if these are used on the left-hand side of Eq. (54) the results are not necessarily equal to the right-hand side for all \mathbf{p} . To obtain even a rough idea about bag-model values of f_ρ and f_ω , one must employ some approximation procedure.

Many authors, when confronted with such difficulties, have employed wave-packet expansions. The idea is old: project a state of definite three-momentum from the bag state. These projected states are then used to evaluate the desired matrix elements. This procedure is necessarily somewhat arbitrary, since the projected state violates Lorentz invariance. The results obtained are therefore only first estimates and have some uncertainty. In what follows we present and employ two popular procedures.⁴² The difference in the results gives an indication of the uncertainties. What is needed, but not currently available, are Lorentz-invariant bag-model states.

If one employs a wave-packet expansion one may decompose a vector-meson bag centered at a position \mathbf{Z} in the following manner:

$$|V(m), \mathbf{Z}\rangle_B = \int \frac{d^3p}{2\omega_p} \phi(p) \exp(i\mathbf{p} \cdot \mathbf{Z}) |V(\mathbf{p}, m)\rangle, \quad (55)$$

where $\phi(p)/\omega_p$ is a parametrization such that

$$\langle V(\mathbf{p}, m) | V(\mathbf{p}', m') \rangle = \delta_{mm'} (2\pi)^3 \delta(\mathbf{p} - \mathbf{p}') 2\omega_p, \quad (56)$$

the normalization used in (54) with

$$(2\pi)^3 \int d^3p \frac{|\phi(p)|^2}{2\omega_p} = 1. \quad (57)$$

The next step is to determine $\phi(p)$. There is no unique procedure, so ϕ can be any suitably normalized function that vanishes for very large p , has a maximum at near $p=0$ and a width in momentum space governed by the inverse of the bag radius.

Wong's⁴² procedure is to use the inverse of Eq. (56) and the above definitions to show that

$$\phi(p) = [(2\pi)^3 \omega_p I(p)]^{1/2}, \quad (58)$$

$$I(p) = \frac{1}{(2\pi)^3} \int d^3r \exp(-i\mathbf{p}\cdot\mathbf{r})_B \langle V(m), \mathbf{0} | V(m), \mathbf{r} \rangle_B.$$

The next step is to use the expansion in (55) in Eq. (54). Then one obtains expressions for f_ρ, f_ω which turn out to be momentum dependent. After averaging over the wave packet so that the angular dependence of $f_\rho(\mathbf{p}), f_\omega(\mathbf{p})$ drops out, the following expressions were found²⁶ ($p = |\mathbf{p}|$):

$$f_\rho(p)^{-1} = \frac{\sqrt{3}\omega_p}{\sqrt{2}\phi(p)m_\rho^2\pi^2} \times \int_0^\infty r^2 dr j_0(pr) [u^2(r) - \frac{1}{3}l^2(r)], \quad (59a)$$

$$f_\omega(p) = 3f_\rho(p) \frac{m_\omega^2}{m_\rho^2}, \quad (59b)$$

where $u(l)$ are the upper (lower) component of the positive-energy state for the quark-antiquark pair in the vector meson. The definition

$$F(p) = \int_0^\infty r^2 dr j_0(pr) [u^2(r) - \frac{1}{3}l^2(r)] \quad (60)$$

is useful. To simplify the numerical calculation, an approximate quark bag wave function introduced by Duck⁴⁶ was used:

$$\psi(\mathbf{r}) = [R_0^3 \pi^{3/2} (1 + \frac{3}{2}\beta^2)]^{-1/2} e^{-r^2/2R_0^2} \begin{pmatrix} 1 \\ i\beta\boldsymbol{\sigma}\cdot\mathbf{r} \\ R_0 \end{pmatrix}. \quad (61)$$

R_0 is related to the bag radius R by requiring the wave function (61) to reproduce the bag value of the root-mean-square radius and $\beta^2=0.15$ is determined so as to reproduce the observed nucleon axial-vector coupling constant.

Donoghue and Johnson⁴² employ another technique. The quantities f_ρ, f_ω are regarded as constants fixed by the normalization condition (57). That is, one uses (55) in (54) with $f_\rho (f_\omega)$ treated as constants. The use of (57) then gives

$$1 = 24 \frac{(f_\rho^{\text{DJ}})^2}{m_\rho^4} \int p^2 dp \omega_p F^2(p) \quad (62a)$$

and

$$f_\omega^{\text{DJ}} = 3f_\rho^{\text{DJ}} m_\omega^2 / m_\rho^2. \quad (62b)$$

Next we present the numerical results. To evaluate Eq. (59a) one must evaluate f_ρ at some values of p . One may take $p^2 = \langle p^2 \rangle$, which is the expectation value of the square at the momentum in the wave packet $\langle p^2 \rangle = 10.4/R^2$ and $R = R_\rho = R_\omega = 0.92$ fm as derived from the spectroscopic calculation.⁴⁷ Then

$$f_\rho(\langle p^2 \rangle^{1/2}) = 5.4, \quad f_\omega(\langle p^2 \rangle^{1/2}) = 16.8.$$

The evaluation of Eq. (62) gives alternatively

$$f_\rho^{\text{DJ}} = 8.8, \quad f_\omega^{\text{DJ}} = 27.$$

These DJ results are essentially what is obtained by setting $p=0$ in Eq. (59a). The experimental values are

$$f_\rho^{\text{expt}} = 4.9 \pm 0.3, \quad f_\omega^{\text{expt}} = 16.3 \pm 0.8.$$

The cloudy bag model affords a reasonable calculation of the $V \rightarrow \gamma$ transition, but there is considerable uncertainty involved with the projection procedure. This problem surfaces again in the calculations of the $\omega, \rho \rightarrow \pi, \gamma$ widths.

IV. CALCULATION OF THE M1 RADIATIVE TRANSITIONS

A. Introduction

In this section the formalism of Secs. II and III is used to calculate the $M1$ transitions among vector and pseudoscalar mesons. From the discussion in the previous section it follows that the various contributions to the $M1$ mesonic transition arising from our CBM Lagrangian can be expressed by the diagrams of Figs. 1 and 2 where A and B stand for pseudoscalar and vector-meson bags.

In general, the bags appearing in the intermediate states in Figs. 1(b)–1(d) may be different from the bag states A, B . In the present work, limited to the S -state solutions of the $q\bar{q}$ system, we have only the pseudoscalar- and vector-meson bags of the $35 \oplus 1$ multiplet of $SU(6)$ at our disposal. Then the selection rules of strong interactions imply the intermediate bag states are of type A and B only.

There is justification for neglecting intermediate states other than A or B in Figs. 1(b)–1(d). The excitation of high-lying intermediate states is suppressed considerably by including effects of the pion's finite extent, as shown by Crawford and Miller.⁴⁴ Of course, the very lowest of the ignored excited states might make a small contribution. This is discussed below in Sec. V.

When we write the matrix elements for the transitions of Table I using the explicit expressions (44), (45), (49)–(52), and (54)–(59), we find it particularly interesting that one may classify these transitions into three separate groups.

(A) Radiative transitions among mesonic bags, to which only j^Q contributes [Fig. 1(a)]. To this class belong the transitions $V \rightarrow \eta\gamma$, $\eta' \rightarrow V\gamma$, and $\phi \rightarrow \eta'\gamma$, where $V \rightarrow \omega, \phi, \rho$.

(B) Radiative transitions between mesonic bags, to which both j^Q and j^π contribute [Figs. 1(a)–1(d)]. The $K^{*+} \rightarrow K^+\gamma$ and $K^{*0} \rightarrow K^0\gamma$ transitions belong to this class. As in the calculation of Sec. IV C, the π -exchange contribution is of major significance in these decays.

(C) Radiative transitions between a vector-meson bag and a pion, i.e., $\omega, \rho, \phi \rightarrow \pi\gamma$. The transitions arise in the CBM from the diagram of Fig. 2(a).

This classification is a direct result of the detailed dynamical model we use, namely, a chiral bag model endowed with $SU(2) \otimes SU(2)$ symmetry. It should be contrasted with the "traditional" approach to radiative decays, which is basically developed^{4,7–9,17} on the underlying $SU(3)$ symmetry for the magnetic moment inducing

the transitions [or, alternatively, with an SU(3)-based phenomenological Lagrangian^{10-12,15,16}], onto which deviations from SU(3) are superimposed. In our case, the singular role of the pion which is the "working hypothesis" of the CBM, establishes an SU(2)⊗SU(2) symmetry framework.

We turn now to the details of the calculations. One might think that the calculation has several free parameters: the pion-quark coupling constant f_π , the quark masses, and the bag radii. However, f_π is determined in the CBM by the pion lifetime via PCAC ($f_\pi=93$ MeV) and the rest of the parameters were determined in the CBM calculation of the baryon and meson masses. The values of these parameters as determined in the spectroscopic calculation are used in this case. *Thus our calculation is completely parameter free*, as well as consistent with the CBM calculation of particle masses. Thus, we use⁴⁷

$$m_u = m_d = 0, \quad m_s = 218 \text{ MeV}, \quad (63a)$$

$$R_K = R_\eta = R_{\eta'} = 0.79 \text{ fm},$$

$$R_\omega = R_\rho = 0.92 \text{ fm}, \quad (63b)$$

$$R_{K^*} = R_\phi = 0.91 \text{ fm},$$

and consequently

$$\Omega_{u,d} = 2.04, \quad \Omega_s = 2.04 + 0.36m_s R. \quad (63c)$$

B. Transitions involving η, η' mesons

All transitions where one has η or η' bags in the final state or an η' bag in the initial state belong to our class (A). It is easy to see by considering isotopic-spin and charge-conjugation symmetries (or G parity) that no vector or pseudoscalar meson of the lowest multiplets can couple strongly to $\eta'\pi$ or $\eta\pi$. Accordingly, diagrams [Figs. 1(b)–1(d)] are forbidden in this case and these transitions are induced solely by the quark current of Fig. 1(a). The matrix elements between the appropriate bag states are given by (44)–(46).

The V, η, η' spin-isospin wave functions are those of the usual⁴⁸ SU(6) expressions. At this point, we have to specify our treatment of the mixing-angle problem. Both vec-

tor mesons and pseudoscalar mesons must be considered. It is well known that for vector mesons the mixing angle is quite close to the ideal nonet value $\theta_V^0 = 35.3^\circ = \arcsin(1/\sqrt{3})$. This results in a ϕ bag made purely of strange quarks and an ω bag of nonstrange ones, $\omega^0 = \frac{1}{2}(u\bar{u} + d\bar{d})$. In practice, however, one knows that there is a small violation of this value of θ_V^0 since the (nonet-forbidden) $\phi \rightarrow \rho\pi$, $\phi \rightarrow \pi\gamma$ decays do occur. Thus, we adopt here the mixing angle given³ by the quadratic mass formula of $\theta_V = 39^\circ$ and we express our states by using the angle δ_V expressing the deviation from pure nonet states, $\delta_V = \theta_V - \theta_V^0 = 3.7^\circ$. This allows us to calculate $\phi \rightarrow \pi\gamma$. Here this is due to the ability of the small ($u\bar{u} + d\bar{d}$) admixture in the ϕ bag to emit a pion. We do include this correction for all other decays involving ω and ϕ bags.

The mixing angle of the pseudoscalars η, η' may be determined from the quadratic mass formula or from the two-photon decays of the three neutral pseudoscalar mesons π^0, η^0, η'^0 . The first method leads³ to a mixing angle of $\delta_P = -10^\circ$. Using the values given for the two-photon decays by the Particle Data Group,³ one finds $\delta_P = -9.5^\circ \pm 2.0^\circ$. It is convenient^{4,7} to define an $\eta-\eta'$ mixing angle given by $\theta_P = \arcsin(1/\sqrt{3}) - \delta_P$. Given the above values of δ_P , one sees that θ_P is very close to 45° . It is therefore natural to take $\theta_P = \arcsin(1/\sqrt{2})$. The physical η, η' states are then simply given by

$$\begin{aligned} \eta &= \frac{1}{2}(u\bar{u} + d\bar{d} - \sqrt{2}s\bar{s}), \\ \eta' &= \frac{1}{2}(u\bar{u} + d\bar{d} + \sqrt{2}s\bar{s}). \end{aligned} \quad (64)$$

Each contains the same percentage of strange quarks.

It is useful here to observe that a new measurement of $\Gamma_\eta(2\gamma)$, giving $\Gamma_\eta(2\gamma) = 0.56 \pm 0.16$ keV, was recently reported.⁴⁹ The older Cornell experiment⁵⁰ from which the angle $\delta_P = -9.5^\circ$ was deduced gave $\Gamma_\eta(2\gamma) = 0.324 \pm 0.046$ keV. The new value would lead to a mixing angle of $\delta_P = -17.6^\circ \pm 3.6^\circ$ and affect appropriately the calculation. Our numerical results are presented for $\theta_P = 45^\circ$ (which corresponds to the widely accepted value of $\delta_P \simeq -10^\circ$), but we shall list for general reference the expression of the matrix elements as functions of δ_V and θ_P . We give in Table II the value of momentum of the emit-

TABLE II. The matrix elements for the transitions involving η and η' decays. The results presented in Table I are calculated with $\theta_P = 45^\circ$; $\delta_V = 3.7^\circ$.

Transition	Matrix elements	q value (MeV)	Value of μ^{PV} (fm)	Value of μ_s^{PV} (fm)
$\rho \rightarrow \eta\gamma$	$\sqrt{3}\mu^{\rho\eta}\sin\theta_P$	189	0.166	
$\omega \rightarrow \eta\gamma$	$\frac{\mu^{\omega\eta}}{\sqrt{3}}\sin\theta_P\cos\delta_V - \frac{2\mu_s^{\omega\eta}}{\sqrt{3}}\cos\theta_P\sin\delta_V$	199	0.165	0.149
$\phi \rightarrow \eta\gamma$	$\frac{2\mu_s^{\phi\eta}}{\sqrt{3}}\cos\theta_P\cos\delta_V + \frac{\mu^{\phi\eta}}{\sqrt{3}}\sin\theta_P\sin\delta_V$	362	0.135	0.122
$\eta' \rightarrow \rho\gamma$	$\sqrt{3}\mu^{\eta'\rho}\cos\theta_P$	170	0.168	
$\eta' \rightarrow \omega\gamma$	$\frac{\mu^{\eta'\omega}}{\sqrt{3}}\cos\theta_P\cos\delta_V + \frac{2\mu_s^{\eta'\omega}}{\sqrt{3}}\sin\theta_P\sin\delta_V$	159	0.170	0.153
$\phi \rightarrow \eta'\gamma$	$-\frac{2\mu_s^{\phi\eta'}}{\sqrt{3}}\sin\theta_P\cos\delta_V + \frac{\mu^{\phi\eta'}}{\sqrt{3}}\cos\theta_P\sin\delta_V$	60	0.177	0.160

ted photon as well as the numerical values of μ^{PV}, μ_s^{PV} calculated from (44)–(46). μ^{PV} is the quantity of (44) when $i \equiv u, d$ and μ_s^{PV} is the quantity obtained from (44) when $i \equiv s$. The moments of μ^{PV}, μ_s^{PV} differ slightly for the different P, V states, since these depend on the values of bag radii and the available momentum for decay, q . The expressions given in Table II, when used in conjunction with Eqs. (41) and (42), lead to our predictions for these decays, as listed in Table I. For the radius R in (44), we use the average value of the P, V bags involved.

C. Transitions involving K mesons

There are two independent transitions in this class, $K^{*\pm} \rightarrow K^\pm \gamma$ and $K^{*0} \rightarrow K^0 \gamma$, and it is particularly in these transitions that large symmetry breaking is observed. SU(3) flavor symmetry requires the neutral decay mode to be four times larger than the charged one. Although the measurement⁵¹ of the neutral mode has a large uncertainty, its rate is evidently only 1–2 times larger than the more accurately measured⁵² charged mode, which is a strong indication of a large SU(3)-symmetry-breaking effect. This suppression of the neutral K^{*0} mode was in fact predicted¹⁰ a long time ago, from the overall pattern of symmetry breaking in the radiative decays involving η 's.

In our model these decays belong to class (B), which has contributions from all diagrams depicted in Fig. 1. We turn now to the details of the calculation. As mentioned previously, we perform the calculation in the quark basis. All diagrams contributing at the quark level to the K^* radiative decays, in the “one-pion-in-the-air” approximation, are shown in Fig. 3.

The contribution of the quark current (28) [see also Fig. 1(a)], as detailed in Fig. 3(a), is calculated from formulas (44)–(46) and one obtains

$$\mu^{K^{*+}K^+} = \frac{-1}{\sqrt{3}}(2\mu^{K^*K} - \mu_s^{K^*K}), \quad (65a)$$

$$\mu^{K^{*0}K^0} = \frac{1}{\sqrt{3}}(\mu^{K^*K} + \mu_s^{K^*K}), \quad (65b)$$

$$\hat{M}_{K^*K}^Q(q) = i\mu^{VP}(q) \frac{1-\tau_3}{2} \int \frac{d^3k}{(2\pi)^3} \left[\frac{\Omega}{\Omega-1} \right]^2 \frac{j_1^2(kR)}{8f_\pi^2 R^2 \omega_k^3} \{ \sigma \cdot \hat{\mathbf{k}} [\mathbf{q} \cdot (\hat{\boldsymbol{\epsilon}} \times \hat{\boldsymbol{\sigma}})] \sigma \cdot \hat{\mathbf{k}} \},$$

which, after performing

$$\int d\hat{\mathbf{k}} \sigma \cdot \hat{\mathbf{k}} (\sigma \cdot \mathbf{K}) \sigma \cdot \hat{\mathbf{k}} = -\frac{4\pi}{3} \sigma \cdot \mathbf{K}$$

with \mathbf{K} defined in (38) becomes

$$\hat{M}_{K^*K}^Q(q) = i\mu^{K^*K}(q) \left[\frac{1-\tau_3}{2} \right] \sigma \cdot \mathbf{K} \frac{1}{48\pi^2} \left[\frac{\Omega}{\Omega-1} \right]^2 \times \frac{1}{f_\pi^2 R^2} \int_0^\infty j_1^2(kR) \frac{k^2 dk}{\omega_k^3}. \quad (67)$$

Observe that the $\frac{1}{2}(1-\tau_3)$ factor of (67) gives zero when acting on an up quark and is unity for a down quark. This is an expression of the fact that for an up

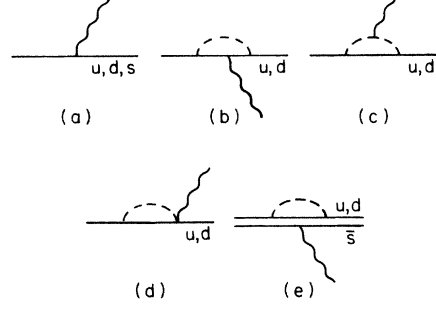


FIG. 3. The contributions to the decays $K^* \rightarrow K \gamma$ at the level of quark diagrams.

where we denote, as before, by μ^{VP} the moment induced by massless u, d quarks and by μ_s^{VP} the part due to the strange quarks. The photon momentum (q value) in these decays is 309 MeV and the explicit evaluation of expression (44) for μ_i^{VP} , using $R^{K^*K} = 0.85$ fm gives

$$\mu^{K^*K} = 0.153 \text{ fm}, \quad \mu_s^{K^*K} = 0.127 \text{ fm}. \quad (66)$$

Figure 3(b) represents radiation also induced by the quark current, while the (u, d) quarks emit and reabsorb a pion. To evaluate this diagram, for which we need Eqs. (19), (23)–(25), and (28), we treat the term of Fig. 3(b) as an operator \hat{M}_{PV}^Q acting on the u and d quarks. [The definition of \hat{M}_{PV}^Q parallels that of Eq. (45).] In employing this procedure, $K^* - K$ energy differences in energy denominators are neglected. Since there are no vanishing energy denominators, this is a reasonable approximation. The matrix element has thus the general form

$$\hat{M} \sim \langle q | H_I^{(q)} | q_n \pi_1 \rangle \frac{1}{\omega_{\pi_1}} \langle q_n \pi | H_{EM}^{(q)} | q_m \pi \rangle \times \langle q_m \pi | H_I^{(q)} | q \rangle$$

with $H_I^{(q)}$ of (23). Evaluating this expression and summing over the charges of the intermediate pions leads to the following expression for $\hat{M}_{K^*K}^Q$:

quark the two terms involving intermediate π^+ and π^0 cancel exactly, while for the down quark there is only partial cancellation. Note also from Eq. (67) that $\hat{M}_{K^*K}^Q$ is essentially given by $M_{K^*K}^Q$ times $P_\pi/9$, where P_π is the probability to have a pion,²¹

$$P_\pi = \frac{3}{16\pi^2} \frac{1}{f_\pi^2 R^2} \left[\frac{\Omega}{\Omega-1} \right]^2 \int \frac{k^2 j_1^2(kR) dk}{\omega_k^3},$$

when intermediate excitation energies are neglected. One should observe that $\hat{M}_{K^*K}^Q$ is included in our general definition (45) of M_{PV}^Q . It is that part of it which has one pion in the air during the quark's interaction with the electromagnetic field. Since P_π is small in the CBM, we

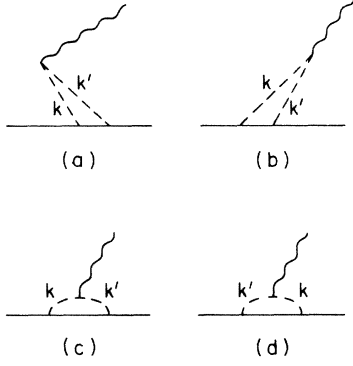


FIG. 4. The four terms obtained by time ordering for the diagram of Fig. 3(c).

expect the term (67) to be very small. Indeed, a numerical evaluation of it shows it to be less than one percent of the term given by Fig. 3(a).

A similar fate is reserved for the term corresponding to Fig. 3(d), which, as we have already remarked, is suppressed to a similar magnitude. As for the term corresponding to Fig. 3(e), it does not contribute at all since it is canceled by renormalization terms. We are thus left with the pionic term of Fig. 3(c). This turns out [along with that of Fig. 3(a)] to be an important term. To evaluate the pionic term we neglect again the K^*-K energy differences in the energy denominators. The pion current operator (33) contains implicitly four terms, corresponding to the time ordering shown in Fig. 4. These terms add coherently to produce a significant effect. Since the photon couples to pions, it affects the isovector part of the transition.

The term to be evaluated, $M_{K^*K}^\pi$, is given in general form in Eqs. (49)–(53). For the case at hand, one has

$$\begin{aligned} \left\langle K^{*+} \left| \sum_{i=1,2} (\sigma_3 \tau_3)_i \right| K^+ \right\rangle &= -\sqrt{3}, \\ \left\langle K^{*0} \left| \sum_{i=1,2} (\sigma_3 \tau_3)_i \right| K^0 \right\rangle &= \sqrt{3}, \end{aligned} \quad (68)$$

where the sum subscript i denotes the quark and antiquark in the kaon. For the integral of (52) we get (using $R_{K^*K} = 0.85$ fm) the value

$$W = 1.36 \text{ fm}^{-1}. \quad (69)$$

We see that the pionic contribution is negative for the $K^{*+} \rightarrow K^+ \gamma$ transition and positive for $K^{*0} \rightarrow K^0 \gamma$, thus adding with the same sign to the quark contribution, an important factor in the good agreement achieved. The total amplitude is thus

$$M_{K^*K} = -\frac{i}{\sqrt{3}} (\hat{\mathbf{e}} \times \mathbf{q})_{m_\gamma} (\mu_{K^*K}^Q + \mu_{K^*K}^\pi). \quad (70)$$

The use of Eqs. (46) and (51) as evaluated in this section [see Eqs. (65), (66), and (69)] in Eq. (41) gives the rate values shown in Table I. It is of interest to remark here, that if we had used only $\mu_{K^*K}^Q$ to calculate the partial widths, the results of 26 keV for $K^{*+} \rightarrow K^+ \gamma$ and 66 keV for $K^{*0} \rightarrow K^0 \gamma$ would be obtained. Thus, the virtual pion contribution is very important in understanding these decays. Without the pion currents, the ratio

$R_K = \Gamma(K^{*0} \rightarrow K^0 \gamma) / \Gamma(K^{*+} \rightarrow K^+ \gamma)$ would be $R_K \simeq 2.5$. The deviation from the symmetry value of 4 is the result of the different values for $\mu_{K^*K}^{K^*K}$ and $\mu_{K^*K}^{K^*K}$ [Eq. (66)] caused by $m_s \neq m_u, m_d$. However, the CBM requires the inclusion of the pion effects whereby $SU(2) \times SU(2)$ symmetry is implemented. With the inclusion of the pionic exchanges, we obtain a further reduction of the ratio to $R_K \simeq 2$. This is in fair agreement with the present experimental value of $R_K = 1.5 \pm 0.8$. Needless to say, the good results we obtain for the absolute values of these partial decay widths are of equal importance.

D. Transitions involving pions in the final state

The class of transitions having pions in the final state is given in the CBM by the diagram of Fig. 2(a). Such transitions are typical of a chiral bag model. Our use of the CBM allows its explicit calculation. We have shown²⁶ that the $\omega\rho\pi$ vertex (as well as the other $VV\pi$ and $VP\pi$ vertices) can be successfully calculated in the CBM and the calculation reproduced the experimentally determined widths within less than 10%. Moreover, it was shown in Ref. 26 that following the procedures of Donoghue and Johnson,⁴² and Wong⁴² of relating the bag state of indefinite momentum to momentum eigenstates by a wave-packet expansion, one can calculate the f_V couplings determining the strength of the electromagnetic transition of a vector-meson bag to a photon.

It should be remarked that our diagram of Fig. 2(a) is reminiscent of the Gell-Mann–Sharp–Wagner (GSW) model¹ of vector dominance for the $\omega \rightarrow \pi\gamma$ decay. However, while in GSW this is an effective phenomenological diagram, which allows one to relate $\omega \rightarrow \pi\gamma$ to $\omega \rightarrow (\rho)\pi \rightarrow 3\pi$, our process of Fig. 2(a) emerges naturally from the CBM Lagrangian to first order in electromagnetism and the quark-pion interaction.

We present now the calculation for $\omega \rightarrow \pi\gamma$. The modes $\rho \rightarrow \pi\gamma$ and $\phi \rightarrow \pi\gamma$ are obtained by the same procedure. In considering these decays, a problem arises from the fact that ω, ρ, ϕ bag states are not momentum eigenstates. The square of the total momentum operator \mathbf{p} does not vanish when acting on $|V\rangle_{\text{bag}}$, so that the π and γ are not necessarily emitted with equal and opposite momenta. The sum of the pion and photon energy is indeed M_V , but there are no other constraints on the momenta. Thus, since transitions that are not really allowed are nevertheless admitted, an overestimate of these partial decay modes is bound to occur.

Instead of obtaining the decay rates directly from the calculated matrix element, as we did for the decays to V , K , and η bags, we proceed to estimate the decays to pions by considering the self-energy term $\Sigma_{V,\pi\gamma}$ of ω, ρ, ϕ due to a pion and γ , from which we extract the partial width by using [see Fig. 2(b)]

$$\Gamma_{V \rightarrow \pi\gamma} = \frac{1}{2} \text{Im} \Sigma_{V,\pi\gamma}. \quad (71)$$

We estimate that this procedure will minimize the effect of the nonallowed states. One should also remark that for transitions to heavy bags like V, η, K this problem is less severe, since these particles have much smaller Compton wavelengths.

The relevant self-energy term is given by

$$\Sigma_{\omega,\pi\gamma} = \frac{1}{(2\pi)^6} \sum_{\alpha} \int \frac{d^3q d^3k}{(2q)(2\omega_k)} \frac{1}{m_{\omega}-q-\omega_k} \frac{1}{(m_{\omega}-m_{\rho}-\omega_k)^2} \left| \sum_{M_{\rho}} \langle \alpha(q) | H_{EM} | M_{\rho} \rangle \langle M_{\rho} | H_{\pi q} | M_{\omega} \rangle \right|^2, \quad (72)$$

where α is the (virtual) photon polarization state, q and k are the momenta of the (intermediate) photon and pion, and M_{ρ}, M_{ω} are the magnetic spin quantum numbers of the intermediate ρ and initial ω mesons. The pion emission matrix element is given by Eqs. (22) and (23) of Ref. 26 and after summing over M_{ρ} and performing the angular integration $d\hat{q} d\hat{k}$ one obtains using Eq. (71)

$$\Gamma_{\omega \rightarrow \pi^0 \gamma} = \frac{1}{24\pi^3} \frac{1}{8f_{\pi}^2 R^2} \int_{m_{\pi}}^{m_{\omega}} \frac{d\omega_k}{\omega_k^2} (\omega_k^2 - m_{\pi}^2)^{1/2} (m_{\omega} - \omega_k) j_1^2 [(\omega_k^2 - m_{\pi}^2)^{1/2} R] F^2(m_{\omega} - \omega_k). \quad (73)$$

$F(q)$ expresses the strength of the vector-meson bag \rightarrow photon transition, which is defined as

$$\begin{aligned} \langle \alpha(q) | H_{EM} | M_{\rho} \rangle &= \hat{\epsilon}_{\alpha} \hat{S}_{\rho} F(q) \\ &= (-1)^{M_{\rho}} \epsilon_{\alpha - M_{\rho}} \delta M_{\rho, \alpha} F(q). \end{aligned} \quad (74)$$

This strength, usually expressed by $f_{\rho}, f_{\omega}, f_{\phi}$ was determined in Ref. 26 where a detailed discussion of its evaluation is presented [see Eqs. (8)–(17) of Ref. 26] and shown to agree well with the value determined from leptonic decay of the vector meson. Using

$$F(q) = \sqrt{3/2} N^2 \int_0^R r^2 dr (j_0^2 - \frac{1}{3} j_1^2) j_0(qR), \quad (75)$$

where N is a known constant [compare to Eq. (13) of Ref. 26], we finally obtain by numerical evaluation $\Gamma_{\omega \rightarrow \pi^0 \gamma} = 1.18$ MeV. The result for $\rho \rightarrow \pi\gamma$ and $\phi \rightarrow \pi\gamma$ is obtained by a similar procedure. The small value of the vector mixing angle, together with the effect of the CBM form factor, combine to give the small value of the $\phi \rightarrow \pi\gamma$ width, which agrees well with experiment.

V. DISCUSSION

A new approach to the calculation of $M1$ radiative transitions among vector and pseudoscalar mesons, based on the formalism of the cloudy bag model is presented here. Our results, summarized in the fifth column of Table I, reproduce remarkably well the available experimental data. The remaining discrepancies are most probably related to the roughness of the present calculation. The inclusion of several corrections is discussed below. Recall also that the experimental figure³ for some of these decays is due to a single measurement. This is the case, for instance, for the $\rho \rightarrow \eta\gamma$ and $\omega \rightarrow \eta\gamma$ decay modes.⁵³ The first of these modes shows indeed the largest apparent discrepancy between our calculation and existing experiment. A glance at the history of the measurements of the $M1$ mesonic transitions reveals that for some of the modes, like $K^{*+} \rightarrow K^+ \gamma$, $\phi \rightarrow \eta\gamma$, the presently available rate (based on several measurements) differs substantially from the result of the first measurement. Thus, it is prudent to compare columns five and six of Table I with these remarks in mind.

Our approach is to use a dynamical model of quarks, gluons and pions, the cloudy bag model, endowed with

$SU(2) \times SU(2)$ symmetry, as opposed to preceding works^{1–11} based on a broken- $SU(3)$ approach. As stressed in the previous sections, we identify three general classes of diagrams (cf. Sec. IV and Figs. 1 and 2) which contribute singly or in combination to the eleven transitions analyzed. The unified picture which $SU(3)_f$ models provide for these decays [though distortions occur because of $SU(3)_f$ breaking], is replaced in our work by the detailed dynamics provided by the Lagrangian of Eq. (17). Decays like $\omega \rightarrow \pi\gamma$ and $\rho \rightarrow \eta\gamma$ or $\omega \rightarrow \eta\gamma$ are no longer related by a Clebsch-Gordan coefficient and arise now from different types of diagrams. The good overall results we obtained are strong indication that these processes belong to a regime^{30,31} where $SU(2) \times SU(2)$ symmetry is a satisfactory symmetry. The large amount of $SU(3)_f$ breaking observed^{1–11} in these decays renders this latter symmetry less useful for the processes at hand, as it is difficult to control the symmetry-breaking pattern in a perturbation-like approach or otherwise. In this respect, we remark that only the nonlinear CBM Lagrangian of Eq. (15) enjoys the full $SU(2) \times SU(2)$ symmetry in the limit of vanishing masses. In practice, we work with a linearized version (17), which is an expansion^{21,37} in the suitably small quantity ϕ/f_{π} . This is different from the chiral perturbation expansions in powers of momenta and masses of quarks,⁵⁴ the relation between the two approaches being still a problem for further study.

In Table I, column four, we give the results obtained for the $M1$ radiative decays by the use of the MIT bag model. Hays and Ulehla¹⁹ were the first to point out that the model fails in this application by nearly an order of magnitude. Hackman *et al.*¹⁹ and Chatley, Singh, and Khanna¹⁹ have extended these calculations to the whole range of radiative decays, after making certain improvements in the basic model. Hackman *et al.* have added a new term to the energy of the bag which allowed them to obtain the correct value for the magnetic moment of the proton, while Chatley, Singh, and Khanna allow for a state-dependent bag pressure. However, when applied to the $M1$ radiative decays, the original Hays-Ulehla results for $M1$ radiative decays were not improved. In Table I we present one of the solutions of Hackman *et al.*, which is typical of the MIT bag results. As shown in this paper, the restoration of chiral symmetry leads to a suitable framework to treat these transitions. A completely new

dynamical picture emerges.

The use of the cloudy bag model, which treats the pion as an elementary field, allows us to incorporate for the first time the effects of the pion cloud in the radiative meson decays. An important conclusion of our work is that *virtual-pion effects* are significant in the $K^* \rightarrow K\gamma$ decays, while they do not affect the $V \rightarrow \pi\gamma$, $V \rightarrow \eta\gamma$, and $\eta' \rightarrow V\gamma$ decays at the level of our approximation, namely, intermediate bag states belonging to the multiplets of vector and pseudoscalar bags and no more than one pion in the air when the photon couples to the bag.^{21,23,24} The virtual pion effects [Figs. 3(b)–3(d)] raise the calculated decay widths obtained from the quark contribution diagram of Fig. 3(a) alone, from 26 to 47 keV for the $K^{*+} \rightarrow K^+\gamma$ mode and from 66 to 98 keV for the $K^{*0} \rightarrow K^0\gamma$ mode. Recall that the exchange current generated by the pion cloud contributes solely to the isovector part of the electromagnetic transition, whose strength is thus sensibly altered by the presence of the pion cloud. In contradistinction, in the transitions belonging to groups (A) ($V \rightarrow \eta\gamma$, etc.) and (C) ($\omega \rightarrow \pi\gamma$, etc.) there are no long-range pion clouds present and the strength of the transition is essentially governed by the quark current (32) matrix elements. The small amount of pion-exchange currents occurring in the transitions of groups (A) and (C), which arises in the presence of high-spin intermediate bags is neglected in our calculation. We shall return to this point shortly.

In principle, there will be a contribution from the pion cloud also to the isoscalar part of the transition. However, this is small since the lowest intermediate state is then due to the emission of three virtual pions annihilating into a photon, which is proportional to $(\phi/f_\pi)^3$ and hence of higher order. The situation for the $M1$ transitions is therefore similar to that encountered in the calculation²⁴ of the baryon magnetic moments, where the pion cloud was also shown to contribute significantly to the isovector part.

At this point, it is natural to inquire about the extension of our approach to $SU(3) \times SU(3)$ symmetry. However, the large difference between the η and K masses on one side and the pion mass on the other side, immediately raises doubts about its applicability in the relatively low-energy regime we investigate. Moreover, one should remember that there is a large intrinsic asymmetry in CBM between the massless u and d quarks and the s quark which comes out to have a mass of 218 MeV. Nevertheless, the extension of the chiral bag models to an $SU(3) \times SU(3)$ -invariant bag has been formally investigated⁵⁵ and such enlarged schemes have been used to estimate the kaon and η -cloud effects to the baryon magnetic moments^{56,57} and to the semileptonic decays of baryons.⁵⁸ Not surprisingly, it was found that these additional contributions do not change appreciably the results obtained with the $SU(2) \times SU(2)$ -symmetric model. This reinforces our view that for the low-energy processes under study, the latter is the relevant and dominant symmetry.

There are several corrections to our approach which ought to be included and which might change the results by 10–15%. However, their inclusion requires further basic studies before truly proved calculations are feasible.

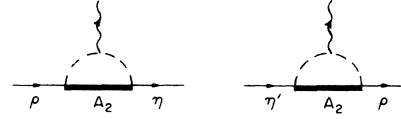


FIG. 5. Pion-cloud diagrams in the decays $\rho \rightarrow \eta\gamma$ and $\eta' \rightarrow \rho\gamma$ involving high-spin intermediate bags (A_2).

We only mention some general points here. First, there is the question of the higher-spin excited states. In our calculations, the intermediate particles were taken to be pseudoscalar and vector bags. The higher-spin intermediate states, like the spin-parity- 2^+ tensor mesons are also possible intermediate states. Their inclusion will allow us to treat the supposedly small effects due to the pion cloud, in decays belonging to class (A) ($V \rightarrow \eta\gamma$ and $\eta' \rightarrow V\gamma$). In Fig. 5 we indicate the diagrams which provide for the inclusion of the pion-cloud effects in the modes $\rho \rightarrow \eta\gamma$ and $\eta' \rightarrow \rho\gamma$.

The inclusion of these diagrams requires the development of the adequate formalism for the vertices containing tensor-meson bags. Such 2^+ states are solutions of the MIT bag static equation with the quark-antiquark system in an $S_{1/2}P_{3/2}$ state. From previous work⁵⁹ one knows that there are difficulties in extending the bag model to the excited states, particularly concerning the number of states and their location. Nevertheless, it is possibly of relevance that the decays $\rho \rightarrow \eta\gamma$ and $\eta' \rightarrow \rho\gamma$, the only ones of class (A) which acquire pion clouds when 2^+ intermediate bags are included, are those which show the largest discrepancy between the CBM calculation and experiment. The inclusion of the pion-cloud effect is expected to ameliorate this.

Two other corrections which might be included are the renormalization of the wave function and of the vertices and the center-of-mass correction. In the CBM, the physical particles are “dressed” bags. Because of the coupling to the pion field, the physical $|\omega\rangle$, for example, will be part of the time (Z_ω) a bare quark-antiquark $|\omega\rangle_0$ state and part of the time will be a bare $|\rho\rangle_0$ bag with one pion in the air, etc. In addition to the wave-function renormalization thus required, there is also an appropriate renormalization (Z_{AB}) of the $VV\pi$ and $VP\pi$ vertices. We calculated the wave-function-renormalization factors Z_ρ, Z_V and vertex-renormalization factor ($Z_{\omega\rho}$ for the $\omega\rho\pi$ vertex, Z_{K^*K} for the $K^*K\pi$ vertex, etc.) using the detailed formalism (for baryons) of Refs. 21, 23, and 24. We find that in all cases of interest here ($Z_\rho, Z_\omega, Z_{K^*}, Z_K, Z_{\omega\rho}, Z_{K^*K}, Z_{K^*K^*}$), these factors differ from one by a few percent only, in accordance with previous findings^{21,23,24} for baryons.

A more difficult and controversial point is the estimate of center-of-mass corrections. The use of procedures developed in Refs. 44, 60, and 61 has been shown^{24,58,61} to change results for magnetic moments and form factors of baryons by up to 10–15%. It is reasonable to expect that similar shifts will occur in the values we obtained for the $M1$ radiative decays. However, the existing treatments of these corrections are not completely satisfactory. Here we take the position that the results presented in Table I are the unambiguous predictions of the “first-order” CBM,

namely, within the working approximation of the model we described (i.e., linearization, one pion in the air, pseudoscalar and vector bags in the intermediate states only, etc.). Corrections to our results, which we enumerated above, should preferably be treated together in order to achieve a reliable estimate of their combined effect on the "first-order" results.

To conclude, we reemphasize that the use of the cloudy bag model, which provides a calculational framework for implementing a chiral $SU(2) \times SU(2)$ QCD model including the pion-cloud effects, leads to a satisfactory treatment of the eleven possible radiative transitions among pseudoscalar and vector mesons. There are certain corrections which we analyzed in this section and which will possibly shift our results to some extent, of the order of 10–15%. In particular, we have some understanding of the major deviations from experiment which we encountered in our calculation. Our treatment of the $\omega, \rho, \phi \rightarrow \pi\gamma$ decays allows for the inclusion of transitions which do not actually occur, thus overestimating somewhat the rates. On the other hand, our inability to treat the intermediate

excited bags, like the spin- 2^+ meson A_2 , leaves out a pion-cloud contribution to $\rho \rightarrow \eta\gamma$ and $\eta' \rightarrow \pi\gamma$ which hopefully will close the gap with experiment.

We conclude with a strong appeal for an experimental effort to measure these transitions with improved accuracy. This will provide an inducing factor for the detailed calculation required for the inclusion of those effects neglected in the present work.

ACKNOWLEDGMENTS

The work of G.A.M. was supported in part by the U.S. Department of Energy and the work of P.S. was supported in part by the Vice President for Research Fund and by the Fund for Promotion of Research at the Technion. This collaboration began when both authors were visitors of the CERN Theory Group and the CERN hospitality is gratefully acknowledged. We are indebted to C. Schmid, G. Eilam, J. Rosner, and L. Wolfenstein for stimulating discussions.

- ¹M. Gell-Mann, D. Sharp, and W. G. Wagner, *Phys. Rev. Lett.* **8**, 261 (1962).
- ²L. M. Brown and P. Singer, *Phys. Rev. Lett.* **8**, 155 (1962); **8**, 353(E) (1962).
- ³Particle Data Group, *Rev. Mod. Phys.* **56**, S1 (1984).
- ⁴P. J. O'Donnell, *Rev. Mod. Phys.* **53**, 673 (1981).
- ⁵C. Becchi and G. Morpurgo, *Phys. Rev.* **140**, B687 (1976); V. V. Anisovich *et al.*, *Phys. Lett.* **16**, 194 (1965); W. E. Thirring, *ibid.* **16**, 335 (1965); L. D. Soloviev, *ibid.* **16**, 345 (1965).
- ⁶G. Morpurgo, *Physics* **2**, 95 (1965).
- ⁷N. Isgur, *Phys. Rev. Lett.* **36**, 1262 (1976); S. Ono, *Phys. Rev. D* **27**, 1203 (1983).
- ⁸R. B. Teese and R. Settles, *Phys. Lett.* **87B**, 111 (1979).
- ⁹D. A. Geffen and W. Wilson, *Phys. Rev. Lett.* **44**, 370 (1980).
- ¹⁰L. M. Brown, H. Munczek, and P. Singer, *Phys. Rev. Lett.* **21**, 707 (1968); P. Singer, *Phys. Rev. D* **1**, 86 (1970).
- ¹¹A. Kotlewski *et al.*, *Phys. Rev. D* **8**, 348 (1973).
- ¹²B. J. Edwards and A. N. Kamal, *Phys. Rev. Lett.* **36**, 241 (1976).
- ¹³S. Gasiorowicz and D. A. Geffen, *Rev. Mod. Phys.* **41**, 531 (1969).
- ¹⁴M. Muraskin and S. L. Glashow, *Phys. Rev.* **132**, 482 (1963).
- ¹⁵B. J. Edwards and A. N. Kamal, *Ann. Phys. (N.Y.)* **102**, 252 (1976); *Phys. Rev. D* **15**, 2019 (1977).
- ¹⁶L. M. Brown and P. Singer, *Phys. Rev. D* **15**, 3484 (1977).
- ¹⁷T. Ohshima, *Phys. Rev. D* **22**, 707 (1980).
- ¹⁸A. Chodos *et al.*, *Phys. Rev. D* **9**, 3471 (1974); T. DeGrand *et al.*, *ibid.* **12**, 2060 (1975); J. Donoghue, E. Golowich, and B. Holstein, *ibid.* **12**, 2875 (1975).
- ¹⁹P. Hays and M. V. K. Ulehla, *Phys. Rev. D* **13**, 1339 (1976); R. H. Hackman *et al.*, *ibid.* **18**, 2537 (1978); P. K. Chatley, C. P. Singh, and M. P. Khanna, *ibid.* **29**, 96 (1984).
- ²⁰A preliminary account on this work was presented in G. A. Miller and P. Singer, *Phys. Lett.* **154B**, 75 (1985).
- ²¹G. A. Miller, S. Th  berge, and A. W. Thomas, *Comments Nucl. Part. Phys.* **10**, 101 (1981); S. Th  berge, A. W. Thomas, and G. A. Miller, *Phys. Rev. D* **22**, 2838 (1980); **23**, 2106(E) (1981); A. W. Thomas, S. Th  berge, and G. A. Miller, *ibid.* **24**, 216 (1981); S. Th  berge, G. A. Miller, and A. W. Thomas, *Can. J. Phys.* **60**, 59 (1982); S. Th  berge, Ph.D. thesis, University of British Columbia, 1982.
- ²²A. Chodos and C. B. Thorn, *Phys. Rev. D* **12**, 2733 (1975); T. Inoue and T. Maskawa, *Prog. Theor. Phys.* **54**, 1833 (1975); C. de Tar, *Phys. Rev. D* **24**, 752 (1981); **24**, 762 (1981); G. E. Brown and M. Rho, *Phys. Lett.* **82B**, 177 (1979); G. E. Brown, M. Rho, and V. Vento, *ibid.* **94B**, 383 (1979); **97B**, 423 (1980).
- ²³A. W. Thomas, *Adv. Nucl. Phys.* **13**, 1 (1984); see also G. A. Miller, in *Quarks and Nuclei*, edited by W. Weise (World Scientific, Singapore, 1984), Vol. 1, p. 189.
- ²⁴S. Th  berge and A. W. Thomas, *Nucl. Phys.* **A393**, 252 (1983).
- ²⁵G. E. Brown and F. Myhrer, *Phys. Lett.* **128B**, 229 (1983).
- ²⁶G. A. Miller and P. Singer, *Phys. Lett.* **130B**, 98 (1983).
- ²⁷A. De R  jula, H. Georgi, and S. L. Glashow, *Phys. Rev. D* **12**, 147 (1975); H. J. Lipkin, *Phys. Rev. Lett.* **41**, 1629 (1978).
- ²⁸H. J. Lipkin, *Phys. Rev. D* **24**, 1437 (1981); see also J. Franklin, *ibid.* **29**, 2648 (1984).
- ²⁹G. E. Brown, M. Rho, and V. Vento, *Phys. Lett.* **97B**, 423 (1980); G. E. Brown, in *High Energy Physics and Nuclear Structure*, proceedings of the Ninth International Conference, Versailles, 1981, edited by P. Catillon, P. Radvanyi, and M. Porneuf [*Nucl. Phys.* **A374**, 63c (1982)].
- ³⁰M. Gell-Mann, R. J. Oakes, and B. Renner, *Phys. Rev.* **175**, 2195 (1968).
- ³¹H. Pagels, *Phys. Rep.* **16**, 219 (1975).
- ³²J. J. Kokkedee, *The Quark Model* (Benjamin, New York, 1969).
- ³³R. Brockman, W. Weise, and E. Werner, *Phys. Lett.* **122B**, 201 (1983).
- ³⁴K. Johnson, in *High Energy Physics and Nuclear Structure* (Ref. 29) [*Nucl. Phys.* **A374**, 51c (1982)].
- ³⁵S. Brodsky and G. P. Lepage, *Phys. Scr.* **23**, 945 (1981).
- ³⁶M. Gell-Mann and M. L  vy, *Nuovo Cimento* **16**, 53 (1960).
- ³⁷R. L. Jaffe, in *Pointlike Structure Inside and Outside Hadrons*, proceedings of the Seventeenth International School of Sub-nuclear Physics, Erice, 1979, edited by A. Zichichi (Plenum, New York, 1982).

- ³⁸G. A. Miller, in *Quarks and Nuclei* (Ref. 23); A. W. Thomas, in *Mesons, Isobars, Quarks, and Excitations*, proceedings of the International School of Subnuclear Physics, Erice, 1983 [Progress in Particle and Nuclear Physics, edited by D. Wilkinson (Pergamon, London, 1984)].
- ³⁹A. Szymacha and S. Tatur, *Z. Phys. C* **7**, 311 (1981).
- ⁴⁰A. W. Thomas, *J. Phys. G* **7**, L283 (1981).
- ⁴¹S. Weinberg, *Physica* **96A**, 327 (1979); *Phys. Rev. Lett.* **18**, 188 (1967).
- ⁴²C. W. Wong, *Phys. Rev. D* **24**, 1416 (1981); J. F. Donoghue and K. Johnson, *ibid.* **21**, 1975 (1980).
- ⁴³M. A. Morgan, Ph.D. thesis, University of Washington, 1984; M. A. Morgan, G. A. Miller, and A. W. Thomas, *Phys. Rev. D* (to be published).
- ⁴⁴G. A. Crawford and G. A. Miller, *Phys. Lett.* **132B**, 173 (1983); M. Araki and A. N. Kamal, *Phys. Rev. D* **29**, 1345 (1984).
- ⁴⁵I. Duck, *Phys. Lett.* **64B**, 163 (1976).
- ⁴⁶I. Duck, *Phys. Lett.* **77B**, 223 (1978).
- ⁴⁷J. Mulders and A. W. Thomas, *J. Phys. G* **9**, 1159 (1983).
- ⁴⁸F. E. Close, *An Introduction to Quarks and Partons* (Academic, London, 1979).
- ⁴⁹A. Weinstein *et al.*, *Phys. Rev. D* **28**, 2896 (1983); another recent experiment performed at the DESY storage ring PETRA by the JADE Collaboration gives also $\Gamma_{\eta}(2\gamma)=0.53\pm 0.08$ keV [DESY Report No. 85-033 (unpublished)]. In these experiments the radiative η -meson width is measured in photon-photon collisions, while in the older experiments (Ref. 50) the Primakoff effect in photoproduction was utilized.
- ⁵⁰A. Browman *et al.*, *Phys. Rev. Lett.* **32**, 1067 (1974).
- ⁵¹W. C. Carithers *et al.*, *Phys. Rev. Lett.* **35**, 349 (1975).
- ⁵²C. Chandler *et al.*, *Phys. Rev. Lett.* **54**, 168 (1983).
- ⁵³D. E. Andrews *et al.*, *Phys. Rev. Lett.* **38**, 198 (1977).
- ⁵⁴J. Gasser and H. Leutwyler, *Phys. Rep.* **87C**, 77 (1982).
- ⁵⁵P. Gonzales and V. Vento, *Nucl. Phys.* **A407**, 349 (1983).
- ⁵⁶P. Gonzales, V. Vento, and M. Rho, *Nucl. Phys.* **A395**, 446 (1983).
- ⁵⁷P. Zenczykowski, *Phys. Rev. D* **29**, 577 (1984).
- ⁵⁸Y. Kohyama *et al.*, Johns Hopkins University Report No. HET 8404, 1984 (unpublished).
- ⁵⁹See, e.g., T. A. DeGrand and R. J. Jaffe, *Ann. Phys. (N.Y.)* **100**, 425 (1976).
- ⁶⁰I.-F. Lan and D. W. Wong (unpublished).
- ⁶¹J. Bartelski *et al.*, *Phys. Rev. D* **29**, 1035 (1984).
- ⁶²There are two new experiments which are not yet included in the values of Table I as given by the Particle Data Group (Ref. 3): (I) A new precise measurement performed at Fermilab [B. Winstein *et al.* (private communication)] gives $\Gamma(K^{*0}\rightarrow K^0\gamma)=118.5\pm 8.1$ keV. We are grateful to Professor Winstein for communicating this result to us in advance of publication. (II) A recent measurement of the product $\Gamma(\eta'\rightarrow\gamma\gamma)B(\eta'\rightarrow\rho\gamma)$ by the PLUTO Collaboration at PETRA [Ch. Berger *et al.*, *Phys. Lett.* **142B**, 125 (1984)], combined with the known values for the branching ratios $B(\eta'\rightarrow\rho\gamma)=(30.0\pm 1.6)\%$ and $B(\eta'\rightarrow\gamma\gamma)=(1.9\pm 0.2)\%$ (Ref. 3), leads to a new value for the $\eta'\rightarrow\rho\gamma$ mode, i.e., $\Gamma(\eta'\rightarrow\rho\gamma)=60\pm 13$ keV. These new data have still to be averaged with previous results (Table I), but both measurements contribute to bring the figures in column six of Table I into closer agreement with our predictions.